20078 년 2 월

박사학위논문

Effects of Hesperidin or Epigallocatechin gallate on the Oral Bioavailability of Verapamil in Rats

조선대학교 대학원

약학과

윤 재 경

Effects of Hesperidin or Epigallocatechin gallate on the Oral Bioavailability of Verapamil in Rats

흰쥐에서 헤스페리딘 또는 에피게로카테친이 베라파밀의 절대경구생체이용율에 미치는 영향

2008 년 2 월 23 일

조선대학교 대학원

약학과

윤 재 경

Effects of Hesperidin or Epigallocatechin gallate on the Oral Bioavailability of Verapamil in Rats

지도교수 최 준 식

이 논문을 약학박사학위신청 논문으로 제출함.

2007 년 10 월

조선대학교 대학원

약학과

윤 재 경

윤재경의 박사학위논문을 인준함

위원장	서울대학교	교수	이명걸	인
위 원	전남대학교	교수	이용복	인
위 원	조선대학교	교수	최후균	인
위 원	조선대학교	교수	한효경	인
위 원	조선대학교	교수	최준식	인

2007 년 12 월

조선대학교 대학원

Part Ⅰ Effects of Hesperidin on the Oral Bioavailability of Verapamil in Rats

Part Ⅱ Effects of Epigallocatechin gallate on the Oral Bioavailability of Verapamil in Rats

List of Tables

List of Figures

Abstract

Effects of Hesperidin or Epigallocatechin gallate on the Oral Bioavailability of Verapamil in Rats

Jae Kyung Yun
Advisor: Prof. Jun-Shik Choi, Ph.D.
College of Pharmacy,
Graduate School of Chosun University

Favonoids can modulate the P-glycoprotein (P-gp) and microsomal cytochrome P450 isoenzymes (CYP) 3A. The F of many drugs are low which contirbute highly to the first-pass effect mainly caused by phase 1 and phase 2 metabolism, and the members of ATP-binding cassettte (ABC) superfamily mediated-efflux by P-gp in the intestine and the liver. Thuse this study investigated the pharmacokinetics of intravenous (i.v.) or oral verapamil in rats in order to examine the effects of P-gp and CYP 3A by hesperidin or epigallocatechin gallate (EGCG) on the absolute oral bioavailability of verapamil. Hesperidin and epigallocatechin gallate (EGCG), flavonoids, are suggested to inhibit P-gp and CYP3A *in vitro*. A single i.v. (3 mg/kg) or oral (9 mg/kg) dose of verapamil was administered to rats with or without oral adminitration of hesperidin or EGCG at a dose of 3 or 15 mg/kg, respectively, 30 min prior to the oral administration of verapamil. Plasma concentrations of verapamil and norverapamil well determined using an HPLC analysis with a fluorescence detector.

Hesperidin caused significantly ($p < 0.01$) greater the total area under the plasma concentration–time curve (AUC) of verapamil by 71.1–96.8% and the peak concentration (C_{max}) of verapamil by 98.3–105.2%, and the presence of hesperidin was increased the terminal half-life ($t_{1/2}$) of verapamil but not significantly. Hesperidin significantly ($p < 0.01$) decreased the total plasma clearance (CL/F) of verapamil by 41.6–49.2% in rats. However there was no significant change in the time to reach the peak plasma

concentration (T_{max}) and the elimination rate constant (K_{el}) of verapamil by hesperidin.

The AUC and C_{max} of norverapamil were significantly ($p < 0.05$) higher by hesperidin and the presence of hesperidin was increased the terminal half-life ($t_{1/2}$) of verapamil but not significantly, but hesperidin decreased the metabolite-parent ratio (MR) of norverapamil. There was no significant change in the T_{max} and the K_{el} of norverapamil by hesperidin.

EGCG caused significantly ($p < 0.01$) greater the AUC of verapamil by 85.2–127% and the C_{max} by 102–136%, and the presence of EGCG was increased the $t_{1/2}$ of norverapamil but not significantly. The presence of EGCG significantly ($p < 0.01$) decreased the CL/F of verapamil by 46.0–55.9%. The enhanced oral bioavailability of verapamil might be due to the decreased efflux and metabolism of verapamil in the intestine. There was no significant change in the T_{max} and the K_{el} of norverapamil by EGCG.

Compared to the oral control group, the presence of EGCG significantly ($p < 0.05$) increased the AUC of norverapamil by 72.9–93.9% and the C_{max} by 65.3–72.9%, and the presence of EGCG was increased the $t_{1/2}$ of norverapamil, but the metabolite-parent ratio (MR) of norverapamil by EGCG decreased but is not significantly. There was no significant change in the T_{max} and the K_{el} of norverapamil by EGCG.

The enhanced F of verapamil was observed in rats in combination by natural flavonoids, hesperidin or EGCG in this study. It is possible that these natural flovonoids could act as candidates of modulators of P-gp and/or CYP3A to improve the F of verapamil in humans. The pharmacokinetic interaction between verapamil and hesperidin or EGCG should be taken into consideration in the clinical setting.

Key words: Verapamil, Norverapamil, Hesperidin, Epigallocatechin gallate (EGCG), Pharmacokinetics, Bioavaialbility, P-gp, CYP3A, Rats.

국 문 초 록

흰쥐에서 헤스페리딘 또는 에피게로카테친이 베라파밀의 경구생체이용율에 미치는 영향

윤 재 경

지 도 교 수: 최 준 식

조선대학교 대학원 약학과

플라보노이드류의 약물은 P-당단백질과 사이토크롬 P450 3A 을 조절할수 있다. 소장과 간에 존재하는 1 상 및 2 상반응의 대사효소(특히 CYP3A) 및 ATP-binding cassette(ABC) 수송체(특히 P-당단백질)등의 초회통과효과가 경구투여된 약물들의 낮은 생체내이용율의 주요원인이다. 본 실험에서는 베라파밀을 정맥 및 경구로 투여하여 베라파밀의 약물동태학적 파라메타를 연구 검토하였으며 P-당단백질과 CYP3A 에 대해 억제작용이 있는것으로 아려진 헤스페리딘과 에피게로카테친(EGCG)을 동시에 경구투여함으로서 베라파밀의 생체이용율 및 약물동태학적 파라메타의 변화를 연구 검토하였다. 헤스페리딘과 에피게로카테친을 각각 3 및 15 mg/kg 을 경구투여한 30 분 후에 베라파밀(9 mg/kg)을 실험용 흰쥐에 경구투여하였다. 혈장중 베라파밀 및 노르베라파밀의 약물농도는 형광검출기를 사용한 HPLC 로 측정하였다.

베라파밀을 단독 투여한 대조군에 비해 헤스페리딘(3 및 15 mg/kg)과 병용 투여군에서는 베라파밀의 혈장곡선하면적(AUC)은 유의성($p < 0.01$) 있게 71.1-96.8% 증가하였으며 최고혈중농도(C_{max})은 유의성($p < 0.01$) 있게 98.3-105.2% 증가하였다. 대조군에 비해 베라파밀의 반감기($t_{1/2}$)는 헤스페리딘 병용 투여군에서 증가하였지만 유의성 있는 변화가 없었다. 대조군에 비해 헤스페리

딘 병용투여군에서 베라파밀의 토탈클리어런스(CL/F)는 유의성($p < 0.01$) 있게 41.6-49.2% 감소하였다. 헤스페리딘(3 및 15 mg/kg) 병용투여군에서 베라파밀의 절대적생체이용율(F)는 7.9-9.0 로 대조군(4.6%)에 비해 유의성($p < 0.05$) 있게 증가하였다. 헤스페리딘(3 및 15 mg/kg) 병용투여군에서 베라파밀의 상대적생체이용율(RB)는 대조군에 비해 1.71-1.96 배 증가하였다. 대조군에 비해 헤스페리딘 병용투여군에서 베라파밀의 최고혈중농도 도달시간(T_{max}) 및 소실속도정수(K_{el})는 유의성 있는 변화가 없었다.

대조군에 비해 헤스페리딘(3 및 15 mg/kg) 병용투여군에서는 노르베라파밀의 혈장곡선하면적(AUC)은 유의성($p < 0.01$) 있게 67.7-79.3% 증가하였으며 최고혈중농도(C_{max})은 유의성($p < 0.01$) 있게 60.5-64.7% 증가하였다. 대조군에 비해 베라파밀의 반감기 ($t_{1/2}$)는 헤스페리딘 병용투여군에서 증가하였지만 유의성 있는 변화가 없었다. 헤스페리딘(3 및 15 mg/kg) 병용투여군에서 노르베라파밀의 상대적생체이용율(RB)는 대조군에 비해 1.69-1.81 배 증가하였다. 하지만 대조군에 비해 베라파밀의 대사비율(MR)은 감소되였지만 유의성 있는 변화가 없었다. 대조군에 비해 헤스페리딘 병용투여군에서 노르베라파밀의 최고혈중농도 도달시간(T_{max}) 및 소실속도정수(K_{el})는 유의성 있는 변화가 없었다.

베라파밀을 단독 투여한 대조군에 비해 EGCG(3 및 15 mg/kg) 병용투여군에서는 베라파밀의 혈장곡선하면적(AUC)은 유의성($p < 0.01$) 있게 85.2-127% 증가하였으며 대조군에 비해 베라파밀의 최고혈중농도(C_{max})은 유의성($p < 0.01$) 있게 102-136% 증가하였다. 대조군에 비해 베라파밀의 반감기 ($t_{1/2}$)는 EGCG 병용투여군에서 증가하였지만 유의성 있는 변화가 없었다. 대조군에 비해 EGCG 병용투여군에서 베라파밀의 토탈클리어런스(CL/F)는 유의성($p < 0.01$) 있게 46.0-55.9% 감소하였다. EGCG(3 및 15 mg/kg) 병용투여군에서 베라파밀의 절대적생체이용율(F)는 9.52-11.7 로 대조군(5.15%)에 비해 유의성($p < 0.01$) 있게 증가하였다. EGCG(3 및 15 mg/kg) 병용투여군에서 베라파밀의 상대적생체이용율(RB)는 대조군에 비해 1.85-2.27 배 증가하였다. 대조군에 비해 EGCG 병용투여군에서 베라파밀의 최고혈중농도 도달시간(T_{max}) 및 소실속도정수(K_{el})는 유의성 있는 변화가 없었다.

대조군에 비해 EGCG (3 및 15 mg/kg) 병용투여군에서는 노르베라파밀의 혈장곡선하면적(AUC)은 유의성($p < 0.01$) 있게 72.9-93.9% 증가하였으며 대조군에 비해 노르베라파밀의 최고혈중농도(C_{max})은 유의성($p < 0.01$) 있게 65.3-72.9% 증가하였다. 대조군에 비해 베라파밀의 반감기 ($t_{1/2}$)는 EGCG 병용투여군에서 증가하였지만 유의성 있는 변화가 없었다. EGCG(3 및 15 mg/kg) 병용투여군에서 노르베라파밀의 상대적생체이용율(RB)는 대조군에 비해 173-194 배 증가하였다. 대조군에 비해 베라파밀의 대사비율 (MR)은 감소되였지만 유의성 있는 변화가 없었다. 대조군에 비해 EGCG 병용투여군에서 노르베라파밀의 최고혈중농도 도달시간(T_{max}) 및 소실속도정수(K_{el})는 유의성 있는 변화가 없었다.

본 연구에서 흰쥐에게 프라보노이드류인 헤스페리딘 혹은 에피게로카테친을 함께투여 하였을 때 베라파밀 및 노르베라파밀의 생체내이용률을 유의성 있게 증가시켰다. 프라보노이드류들은 천연음식물에 흔이 존재하는 물질로서 인체에서 많은 유익한 작용이 있으며 지속적인 독성작용이 없다. 임상에서 베라파밀을 프라보노이드류인 헤스페리딘 혹은 에피게로카테친이 함유한 음식과 동시에 투여할 경우 약물의 투여량을 조절하는 것이 바람직하다고 사료된다.

Part Ⅰ Effects of Hesperidin on the Oral Bioavailability of Verapamil in Rats

Abstract

Favonoids can modulate the P-glycoprotein (P-gp) and cytochrome P450 (CYP) 3A. The F of many drugs are low which contirbute highly to the first-pass efffect caused mainly by phase 1 and phase 2 metabolism, and the members of ATP-binding cassettte (ABC) superfamily mediated efflux by p-gp in the intestine and the liver. Thus this study investigated the pharmacokinetics of intravenous or oral administration of verapamil in rats in order to examine the effects of CYP3A and/or P-gp by hesperidin on the oral bioavailability of verapamil and one of its metabolites, norverapamil. Hsperidin, flavonoid, are suggested to inhibit P-gp and CYP3A *in vitro*. A single oral (9 mg/kg) dose of verapamil was administered to rats with or without oral administration of hesperidin at a dose of 3 or 15 mg/kg, respectively, was oral administered 30 min prior to the oral administration of verapamil, respectively. Plasma concentrations of verapamil and norverapamil well determined using an HPLC analysis with a fluorescence detector.

Compared to the control group, hesperidin significantly ($p < 0.01$) increased the total area under the plasma concentration–time curve (AUC) of verapamil by 71.1–96.8% and the peak concentration (C_{max}) of verapamil by 98.3–105.2%, and the presence of hesperidin was increased the terminal half-life ($t_{1/2}$) of verapamil but not significantly. Hesperidin significantly ($p < 0.01$) decreased the total plasma clearance (CL/F) of verapamil by 41.6–49.2% in rats. However there was no significant change in the time to reach the peak plasma concentration (T_{max}) and the elimination rate constant (K_{el}) of verapamil by hesperidin.

The AUC and C_{max} of norverapamil were significantly ($p < 0.05$) greater by hesperidin and was increased the terminal half-life ($t_{1/2}$) of verapamil but not significantly, but the metabolite-parent ratio (MR) of norverapamil by hesperidin decreased but is not

significantly. There was no significant change in the time to reach the peak plasma concentration (T_{max}) and the elimination rate constant (K_{el}) of norverapamil by of hesperidin.

The enhanced F of verapamil was observed by hesperidin in this study. It is possible that these natural flovonoid could act as candidates of modulators of P-gp and/or CYP3A to improve the F of verapamil in humans. The pharmacokinetic interaction between verapamil and hesperidin should be taken into consideration in the clinical setting.

Key words: Verapamil, Norverapamil, Hesperidin, Pharmacokinetics, Bioavaialbility, P-gp, CYP3A, Rats.

1. Introduction

The microsomal cytochrome P450 isoenzymes (CYPs) comprise a large group of hemoproteins with monooxygenase activity. They play a major role in the metabolism of numerous xenobiotics, including drugs, carcinogens, pesticides, hydrocarbons, and endogenous compounds, such as steroids. These enzymes are located in various tissues (liver, brain, gut, kidney, and lung) in which several isoenzymes may be expressed simultaneously (Gushchin et al., 1999).

The CYP3A subfamily is the most important to drug metabolism in humans, because they metabolize the majority of commercially available drugs (Wrighton et al., 2000). There are four differentially regulated CYP3A genes in humans, CYP3A4, CYP3A5, CYP3A7 and CYP3A43. CYP3A4 is generally thought to be the predominant form expressed in the liver cells (Wrighton et al., 2000). Recently, it has become apparent that the kinetic interaction between CYP enzymes and their substrates *in vitro* is often atypical, as exemplified by CYP3A4 (Figure 1).

The transport-based classical multi-grug resistance (MDR) is caused by the ATP-binding cassette (ABC) family, a membrane transport ATPases. The general structures of ABC transporters compose of 12 transmembrane (TM) regions, split into two ‘halves’, each with a nucleotide-binding domain (NBD) (Figure 2A), such as P-gp (MDR1), MDR3, BSEP (SP-gp), multidrug resistance-associated protein (MRP) 4, MRP5, and MRP8. The MRP1–3 and MRP6–7 have an additional five TM regions at the N-terminus (Figure 2B). Breast cancer-resistance protein (BCRP) has only six TM regions and one NBD (Figure 2C), which was proposed to function as a dimer (Ozvegy et al., 2001). NDBs play a role in cleaving ATP (hydrolysis) to derive energy necessary for transporting cell nutrients, such as sugars, amino acids, ions and small peptides across membranes.

Althought the overall model of 12 transmembranere regions has been generally well-supported by antibody localization data (Yoshimura et al., 1989), an alternative model has recently appeared based on the coupled *in vitro* translation and translocation of P-gp into dog pancreas microsome membranes (Zhang et al., 1991). This study suggests, based on

the presence of a glycosylated segment in the carboxy-terminal half of P-gp, that under some conditions in mouse P-gp, the eighth and ninth transmembrane domains, and the amino acids between transmembraned omains 8 and 9, might be extracellular rather than cytoplasmic as suggested in the model shown in Figure 2. These results are supported by *in vivo* expression of truncated P-gp chimeras in *Xenopuso* ocytes, as well as by *in vitro* expression of intact human P-gp in a cell-free translation-translocation system (Skach et al., 1993). Howevers, study proteolytic fragments of photoaffinity-labelled P-gp indicates that there does not appear to be a glycosylated region in the carboxy-terminal half of mature human P-gp, arguing against this model of 10 transmembrane regions for a form of P-gp capable of binding drugs (Bruggemann et al., 1989, 1992). However, it is possible that this region is indeed extracellular, but not glycosylated or that P-gp with this variant topology does not survive to the cell surface because of intracellular degradation. The precise topology of P-gp on the mammaliacne ll surface needs further study.

Since the original publication of the human MDR1 and mousem dr3 (mdrla) sequences, full-length sequences have appeared for mouse mdrlb (also called mdr2) (Devault et al., 1990)), mousem dr2 (Gros et al., 1988), human MDR2 (Van der Bliek et al., 1988), hamster p-gpl (similar to mdrla) (Devine et al., 1991), and the rat mdrlb gene (Silverman et al., 1991). Comparison of these sequences shows a considerable amount of sequence identity and homology among mdr family members (Devine et al., 1991). For example, the human MDRI and MDR2 coding sequences are 76% identical despite different abilities to transport drugs, and the mouse mdrla and human MDR1s equences, with similar function, are 88%i dentical, despite 50 million years or moreo fevolution. Amongth e mdr genes that function as multidrug transporters, the regions of greatest homology are the ATP-binding/utilizationr egions, and the first and secondi ntracytoplasmic loops in each half of the molecule. The least conserved regions are the first extracytoplasmic loop, where even glycosylation sites are not preserved, the intracellular linker region.

P-gp is also present at the normal tissues such as kidney and adrenal gland (high level), liver, small intestine, colon and lung (medium level), and prostate, skin, spleen, heart, skeletal muscle, stomach and ovary (low level) (Fojo et al., 1987; Gatmaitan and Arias, 1993). Same as P-gp, MRP1 is highly expressed in intestine, kidney, lung and lower in liver (Cherrington et al., 2002; Flens et al., 1996; Zaman et al., 1993) and MRP2 is

expressed mainly in liver, intestine, and kidney tubules (Fromm et al., 2000; Schaub et al., 1997). As shown in Figure 3, P-gp and MRPs spreaded in the excretory organs provide a barrier to eliminate the substrates out of the body. P-gp and MRP2 co-localized to the apical membrane of the intestine, liver, kidney, and blood-brain barrier (Thiebaut et al., 1987; Buchler et al., 1996; Fromm et al., 2000; Schaub et al., 1999), and MRP1 is localized to the basolateral membranes of polarized epithelial cells of the intestinal crypt (Peng et al., 1999), renal distal and collecting tubules (Peng et al., 1999), and liver (Mayer et al., 1995; Roelofsen et al., 1997).

P-gp and MRPs are reportedly co-localized with phase I and phase II metabolizing enzymes, CYP3A4, UDP-glucuronosyltransferases, and glutathione-*S*-transferases in the liver, kidney and intestine (Sutherland et al., 1993; Turgeon et al., 2001) (Figure 3). The CYP3A subfamily involves in approximately 40–50% of phase I metabolism of marketing drugs (Guengerich, 1995). Specifically, CYP3A4 accounts for 30% of hepatic CYP and 70% of small intestinal CYP (Schuetz et al., 1996). A substantial overlap in substrate specificity exists between CYP3A4 and P-gp (Wacher et al., 1995). Additionally, the phase II conjugating enzymes, such as UDP-glucuronosyltransferases and glutathione-*S*-transferases, may subsequently modify either the phase I metabolites or the parent compounds as the conjugated compounds, and further subject toMRP2-mediated efflux in the liver and intestine. Thus, a synergistic relationship exists between the transporters and metabolic enzymes, such as CYP3A4 versus P-gp and conjugating enzymes versus MRP2, within excretory tissues to protect the body against invasion by foreign compounds, which also decrease the oral bioavailability of many drugs, especially anticancer drugs.

Oral administration of drugs has many advantages over intravenous injection because it is less invasive, easier to use for the patient in a chronic regimen and more cost-effective because of decreased hospitalization. The small intestine represents the principal site of absorption for orally administered compounds. There are two principal pathways, paracellular and transcellular, in the intestinal epithelium that allows the compounds to cross. Some small hydrophilic, ionized drugs are absorbed via the paracellular pathway for there small particle size is suitable for pass through the tight intercellular junctions (Hayashi et al., 1997). Many orally administered drugs are lipophilic and undergo passive transcellular absorption (Hunter and Hirst, 1997). Drugs that cross the apical membrane or

present in the blood would be substrates for apical efflux of transporters, specifically ABC proteins such as P-gp and MRP2, and cytochrome P450 (especially CYP3A4)-mediated Phase I metabolism of orally ingested compounds (Watkins, 1992). Phase I and phase II metabolic enzymes may yield metabolites that are themselves substrates for efflux pumps, such as P-gp and MRP2 (Keppler et al., 1999). The fraction of compounds that escapes this first barrier will pass to the liver via the portal vein and subject to further metabolism and biliary excretion by the same enzymes and transporters present in the enterocytes, which complete the first cycle of enterohepatic circulation (first-pass extraction). Drugs that reach the systemic circulation following first pass extraction by the liver, or through the lymphatics, will meet the kidneys, which are also well equipped with the efflux transporters for the active excretion of the parent or the metabolites of the compounds. The efflux transporters and intracellular metabolic enzymes in the intestine and liver are critical determinants of overall oral bioavailability.

Verapamil is a calcium channel-blocker that is widely used as an antiarrhythmic agent to control supraventricular tachyarrhythmias. Verapamil is also useful for the treatment of hypertension, ischemic heart disease and hypertrophic cardiomyopathy on account of its potent vasodilating and negative inotropic properties (Fleckenstein, 1977; Gould et al., 1982; Lewis et al., 1978). Treatment with verapamil is generally well tolerated, but adverse effcts connected with verapamil is pharmacological effects on cardiac conduction can arise and may be particularly severe in patients with hypertrophic cardiomyopathies. Adverse effects on the heart include bradycardia, atrioventricular block, worsening heart failure, and transient asystole. These effects are more common with parenteral than with oral therapy. The most troublesome non-cardiac adverse effect is constipation. Nausea may occur but is less frequently reported. Other adverse effects include hypotension, dizziness, flushing, headaches, fatigue, dyspnoea, and peripheral oedema. There have been reports of skin reactions and some cases of dbnormal liver function and hepatotoxicity. Gingval hyperplasia has ocurred. Gynaecomastia has been reported rarely (Fleckenstein, 1977; Gould et al., 1982; Lewis et al., 1978).

Verapamil is approximately 90% absorbed from the gastrointestinal tract, but is subject to very considerable first-pass metabolism in the liver and the bioavailability is only about 20%. Verapamil exhibits bi-or tri-phasic elimination kinetics and is reported to have a

terminal plasma half-life of 2 to 8 hours following a single oral dose or after intravenous adnimistration. Verapamil is about 90% bound to plasma proteins (Schomerus et al., 1976). In humans, N-desalkylverapamil (D-617) was the most abundant metabolite in 0-48h urine at a percentage of the excreted dose of 22%, followed by O-desmethyverapamil (D-703; 7%), norverapamil (N-desalkylverapamil; 6%) (Eichelbaum et al., 1979) (Figure 4). Norverapamil is an N-demethylated metabolite of verapamil with approximately 20% of the coronary vasodilating activity of the parent compound in dogs (Eichelbaum et al., 1984). The formation of norverapamil and D-617 was mediated via hepatic microsomal cytochrome P450 (CYP) 3A4 and 1A2, and CYP3A and to a lesser extent, CYP1A2 are the principal mediators of verapamil biotransformation in humans (Levy et al., 2000). Verapamil is a known to be substrate P-gp as well as CYP3A4 (Doppenschmitt et al., 1999; Adachi et al., 2001; Pauli-Magnus et al., 2000; Saitoh and Aungst, 1995). Furthermore, it has been reported that the phase 1 metabolites of verapamil exhibit different P-gp substrate and inhibition characteristics (Hau β ermann et al., 1991; Pauli-Magnus et al., 2000; Woodland et al., 2003). While N-dealkylated metabolites (D-617 and D620) are P-gp substrates, norverapamil and O-demethylated metabolite (D-703) are inhibitors of P-gp function, implying that verapamil metabolites may influence P-gp mediated drug disposition and elimination. P-gp is colocalized with CYP 3A4 at the apical membrane of the cells in the small intestine (Gottesman and Pastan, 1993). Which is a membrane transporter that actively "pumps" xenobiotics out of cells (Doppenschmitt et al., 1999). In the small intestine, P-gp is colocalized with CYP3A4 at the apical membrane of the cells (Gottesman and Pastan, 1993).

Flavonoids are widely distributed in dietary supplements such as vegetables, fruit, tea and wine (Hertog et al., 1993b). Flavonoids have many beneficial effects including antioxidant, antibacterial, antiviral, antiinflammatory, antiallergic, and anticarcinogenic actions (Ross and Kasum, 2002; Hodek et al., 2002) though whether these effects can be attributed to the aglycone forms or their metabolites is not entirely clear. The total daily intake of flavonoids via the dietary supplements has been 23 mg/day in Dutch population (Hertog et al., 1993a), among which the most important flavonoid was the flavonol quercetin (mean intake 16 mg/day). Many flavonoids are ubiquitous in all parts of the plant. Flavonoids are polyphenolic compounds possessing 15 carbon atoms; two benzene

rings joined by a linear three-carbon chain (Figure 5A). A chromane ring bearing a second aromatic ring B in position 2, 3 or 4 (Figure 5B). The oxygen bridge involving the central carbon atom (C_2) of the three-carbon chain occurs in a rather limited number of cases, where the resulting heterocyclic is of the furan type. Various subgroups of flavonoids are classified according to the substitution patterns of ring C. Both the oxidation state of the heterocyclic ring and the position of ring B are important in the classification. The major subgroups of flavonids are as followes (Figure 6): Flavonols (quercetin, morin, kaempferol, myricetin, rutin, isorhamnetin), Flavones (apigenin, luteolin, primuletin), Flavanones (hesperetin, hesperidin, naringenin, naringin, eriodictyol), Flavanols, also called catechins ((+)-catechin, (+)-gallocatechin, (-)-epicatechin, (-)-epigallocatechin, (-)-epicatechin 3-gallate, (-)-epigallocatechin 3-gallate, theaflavin, theaflavin 3-gallate, theaflavin 3'-gallate, theaflavin 3,3'-digallate, thearubigins), Anthocyanidins (cyanidin, delphinidin, malvidin, pelargonidin, peonidin, petunidin) and Isoflavonoids (genistein and daidzein). Most of these (flavanones, flavones, flavonols, and anthocyanins) bear ring B in position 2 of the heterocyclic ring. In isoflavonoids, ring B occupies position 3.

Although there is strong evidence to suggest beneficial effects of flavonoids in human health, the extent and mechanism by which flavonoids reach the systemic circulation from dietary sources are controversial. Plant flavonoids are predominantly found as β-glycosides with flavonols existing as 3, 7, and 4' *O*-glycosides, whereas other flavonoids, such as flavones, flavonones, and isoflavones, are mainly glycosylated at position 7 (Price et al., 1997; Fossen et al., 1998). Dietary flavonoids are deglycosylated by cytosolic β-glucosidase (CBG) and lactase phlorizin hydrolase (LPH) in the small intestine (Day et al., 1998; Day et al., 2000), followed by conjugation primarily with glucuronic acid in the small intestine epithelial cells (Gee et al., 2000; Crespy et al., 1999; Spencere et al., 1999). Ingested flavonoids undergo extensive Phase I and Phase II metabolism and are present in the circulation as a complex mixture of free aglycone with glucuronidated, methylated, and sulphated forms. However, cleavage by glucuronidases at several sites in the body can restore the aglycone form (Figure 3) (Murota and Terao, 2003) of which shows enhanced ability to partition across membranes and access intracellular sites due to its greater lipophilicity (Spencer et al., 2001).

Several studies have shown that flavonoids can modulate the activities of both P-gp and

MRP1 (Zhang and Morris, 2003a; Bobrowska-Hagerstrand et al., 2003) affecting drug accumulation, cell viability following cytotoxic drug exposure, and the ATPase activity of P-gp (Bobrowska-Hagerstrand et al., 2003). Some flavonoids have been reported to interact with the intrinsic ATPase of P-gp, both inhibition and stimulation of P-gp ATPase activity have been observed for silymarin, morin, and biochanin A (Zhang and Morris, 2003b). Since P-gp located in the apical membrane (Anderle et al., 1998) and some mRNAs of organic cation transporters (OCT) has also been detected (Martel et al., 2001), the monolayer formed by a human colon carcinoma cell line, Caco-2 cell, is used for the study of membrane permeability, specifically for the transport characterization of the intestinal epithelium. Some flavonoids reduced the secretory flux of talinolol across Caco-2 cells, such as hesperetin, quercetin, kaempferol, spiraeoside, isoquercitrin and naringin, but none of the selected flavonoids was able to replace [^{3}H]talinolol from its binding to P-gp, which might be due to an interaction with P-gp without competition of talinolol binding site of P-gp (Ofer et al., 2005). Several flavonoids, specifically methoxylated flavonoids, are confirmed to be the good inhibitors of MRP1 and 2 (van Zanden et al., 2004).

Flavonoids comprise a large group of naturally occurring, low molecular weight, polyphenolic compounds widely distributed in the plant kingdom as secondary metabolutes. They represent one of the most important and interesting classes of biologically active compounds and occur both in the free state and as glycodides. They are based on the parent compound, flavone (2-phenyl chromone or 2-phenyl benzopyrone), characterized by a C_6-C_3-C_6 carbon skeleton where the C6 components are aromatic rings (Figure 7). Naringin (4′,5,7-trihydroxyflavanone-7-rhamnoglucoside) and hesperidin (3′,5,7-trihydroxy-4′-methoxyflavanone-7-rhamnoglucoside), also called citrus flavonoids. Flavonoids occur in practically all parts of plants including fruit, vegetables, nuts, seeds, leaves, flowers and bark (Middleton, 1984),

Hesperidin (Figure 8) is an abundant and inexpensive by-product of *Citus* cultivation and is the major flavonoid in sweet orange and lemon. In the young immature oranges it can account for up to 14% of the fresh weight of the fruit (Barthe er al., 1988). It is usually found in association with vitamin C. some symptoms originally thought to be due to vitamin C deficiency such da brusing due to capillary fragility were found in early studies

to be relieved by crude vitamin C extract but not by purified vitamin C. the bioflavonoids, formerly called “vitamin P”, were found to be the essential components in correcting this bruising tendency and improving the permeability and integrity of the capillary lining. These bioflavonoids include hesperidin, citrin, rutin, flavones, flavonols, catechin and quercetin.

Hesperidin is a flavanone glycoside, comprising of and aglycone, hesperetin or methyl eriodictyol (Evans, 1996) and an attached disaccharide, rutinose. Hesperidin is, therefore, a beta-7-rutinoside of hesperetin (Preston et al., 1953). Hesperidin has multiple biological activities such as reduction of capillary fragility, associated with scurvy and antilipedimic activities (Garg et al., 2001; Korthuis and Gute, 1999; Bok et al., 1999; Borradaile et al., 1999). After oral administration, hesperidin is absorbed through the gastrointestinal tract. Of the aglycones, hesperetin has been detected in both urine and plasma, and additional investigation found that absorbed citrus flavanones went through glucuronidation before urinary excretion (Ameer *et al*., 1996). Hesperidin may be regulated by P-gp (Tsai and Liu, 2004).

The flavonoid, hesperidin, was abundant in our dietary supplements. There are many opportunities that these flavonoids would be administered concomitantly with the agents that are substrates for CYP3A and P-gp in the clinical practice. Since they possess the ability to inhibit CYP3A and P-gp, they might affect the pharmacokinetics of many substrate agents. In this study, the pharmacokinetic behavior of verapamil and norverapamil after orally administration of verapamil to rats was investigated the effect of hesperidin on the oral bioavailability of verapamil and norverapamil in rats.

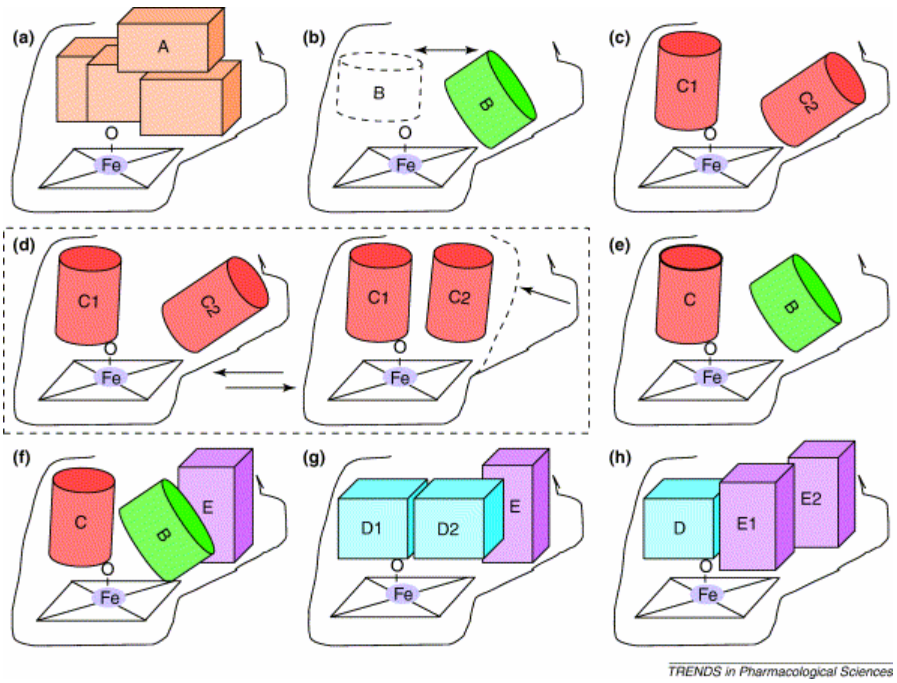

Figure 1. A scheme of the many hypotheses used to describe the binding of ligands to cytochrome P450 3A4 (CYP3A4) (based on [Wrighton et al., 2000]). The solid lines in each panel define the binding pocket that contains the heme and ligands A–E. (a) A single large molecule (A) occupies the whole binding pocket. (b) A molecule (B) could bind in two different locations with the remainder of the active site occupied by water molecules. (c) Two molecules could occupy two unique sites (homotropic activation). (d) Two molecules (C) might bind at two different sites with two or more conformers of the enzyme in equilibrium (nested allosterism). (e) Two different molecules bind to two different sites (heterotropic activation). (f) Three different molecules (C, D and E) bind at different sites, one of these (E) might be an effector. (g) Two identical molecules (D) bind to two sites and the effector (E) binds to a third. (h) Two effector molecules (E) bind and one behaves as a substrate. A third, different, substrate or effector molecule (D) also binds a separate substrate or effector site. When more than one molecule is in the binding pocket, key intermolecular interactions might occur that are not accounted for in this schematic.

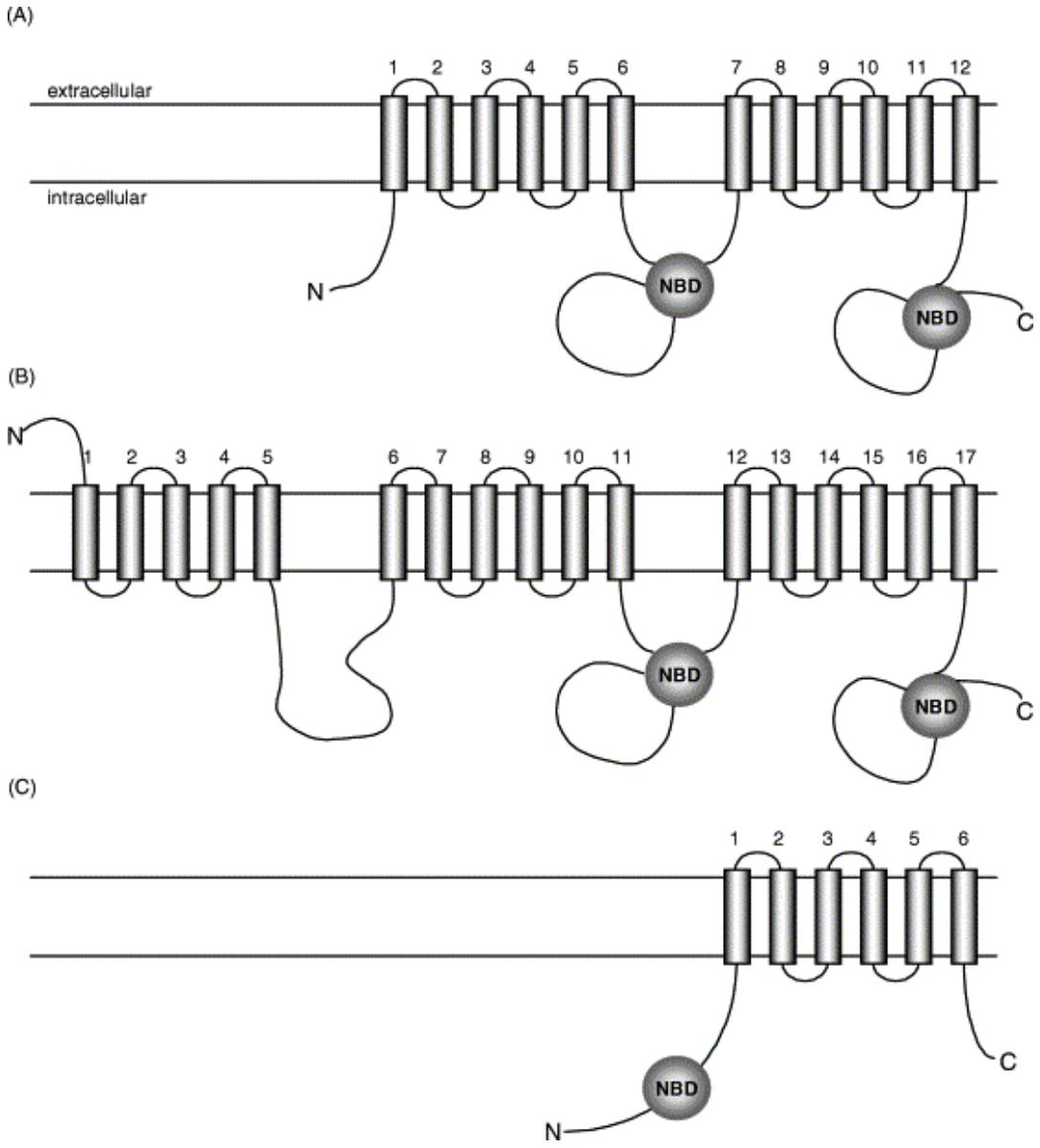

Figure 2. Transmembrane arrangement of ABC efflux proteins. (A) Pgp (MDR1), MDR3, BSEP (SPgp), MRP4, MRP5, and MRP8, have 12 TM (transmembrane) regions and two NBDs (nucleotide binding domains). (B) Typical MRP transporters (MRP1-3 and 6–7) have five extra TM regions towards the N terminus. (C) 'Half-transporters' such as BCRP have just six TM regions and one NBD (Cited from Chan et al., 2004).

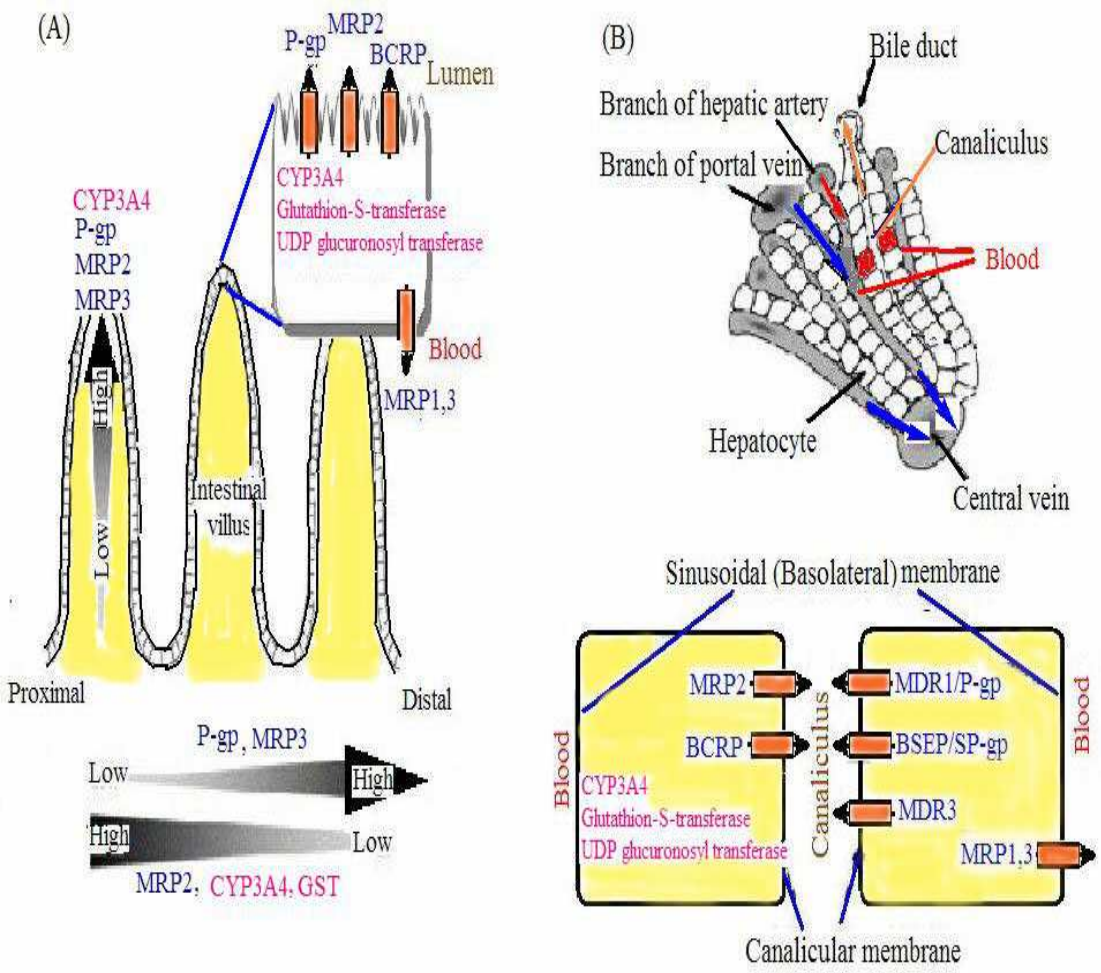

Figure 3. Efflux transporters and intracellular metabolic enzymes in intestinal epithelia (A) and hepatocytes (B).

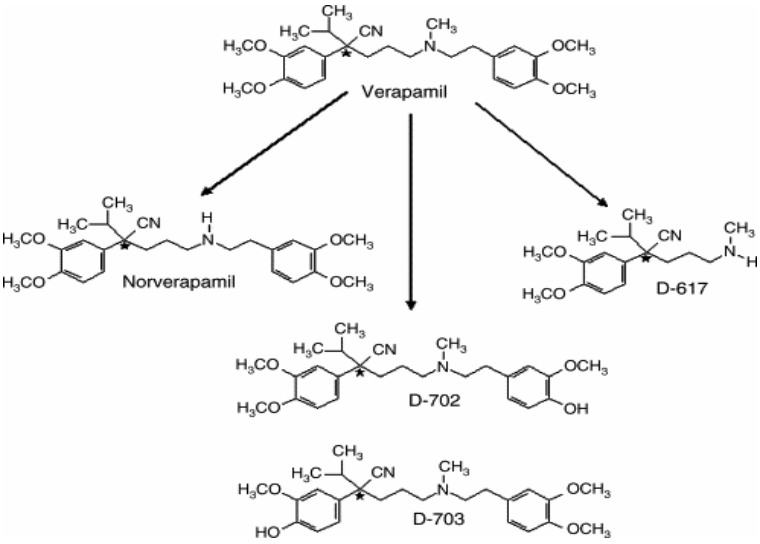

Figure 4. Metabolic pathways of verapamil (Ha et al., 2006)

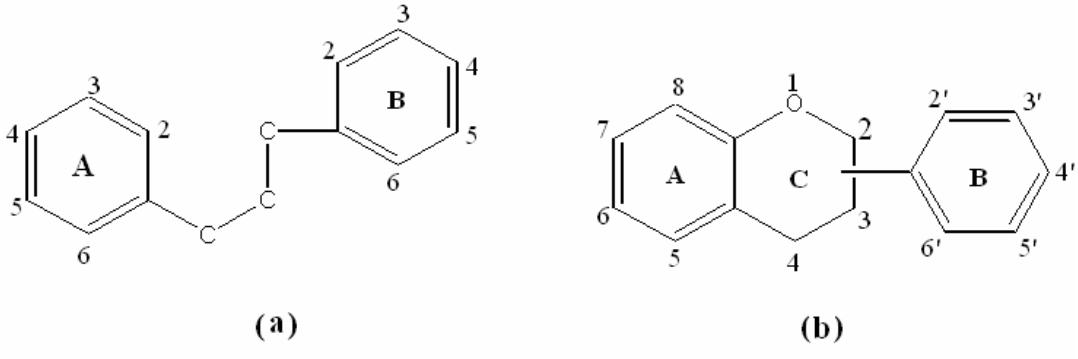

Figure 5. Chemical structures of flavonoids. A C_{15} skeleton can be represented as the C_6-C_3 - C_6 system (a). A chromane ring bearing a second aromatic ring B in position 2, 3 or 4 (b).

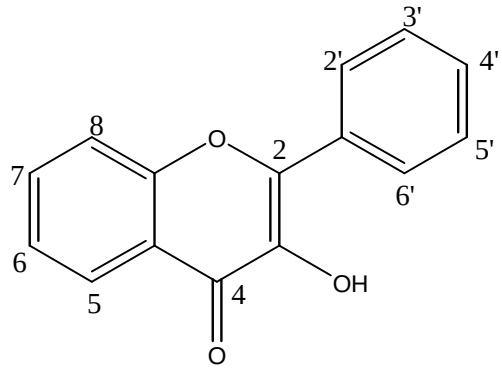

Flavonols

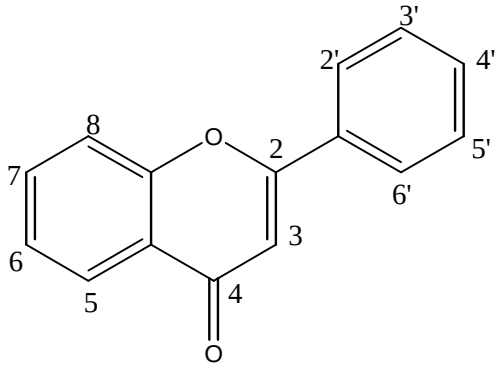

Flavons

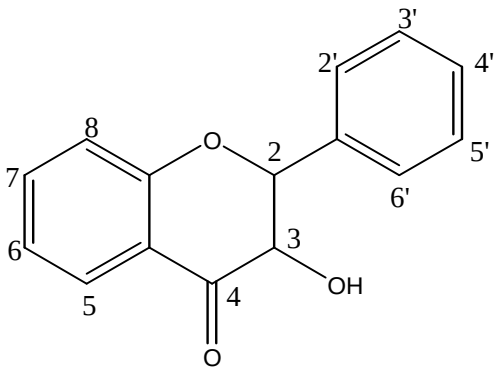

Flavanols

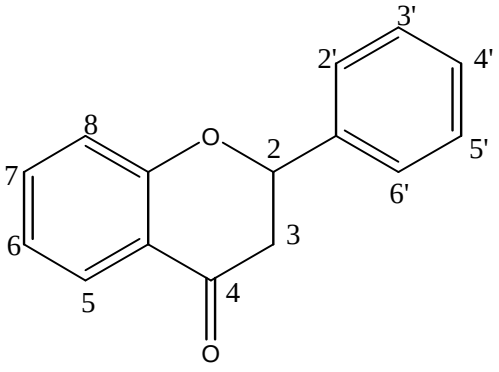

Flavanons

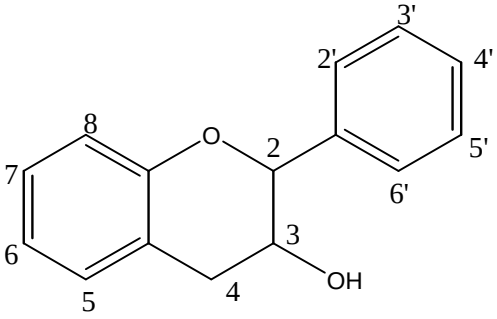

Anthocyanins

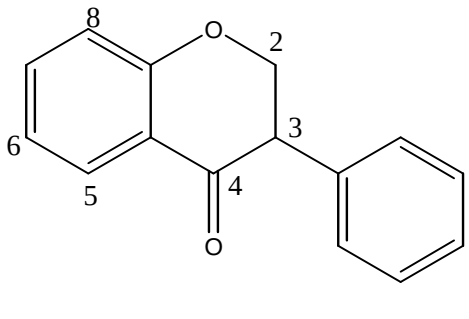

Isoflavonoids

Figure 6. Major subgroups of flavonoids.

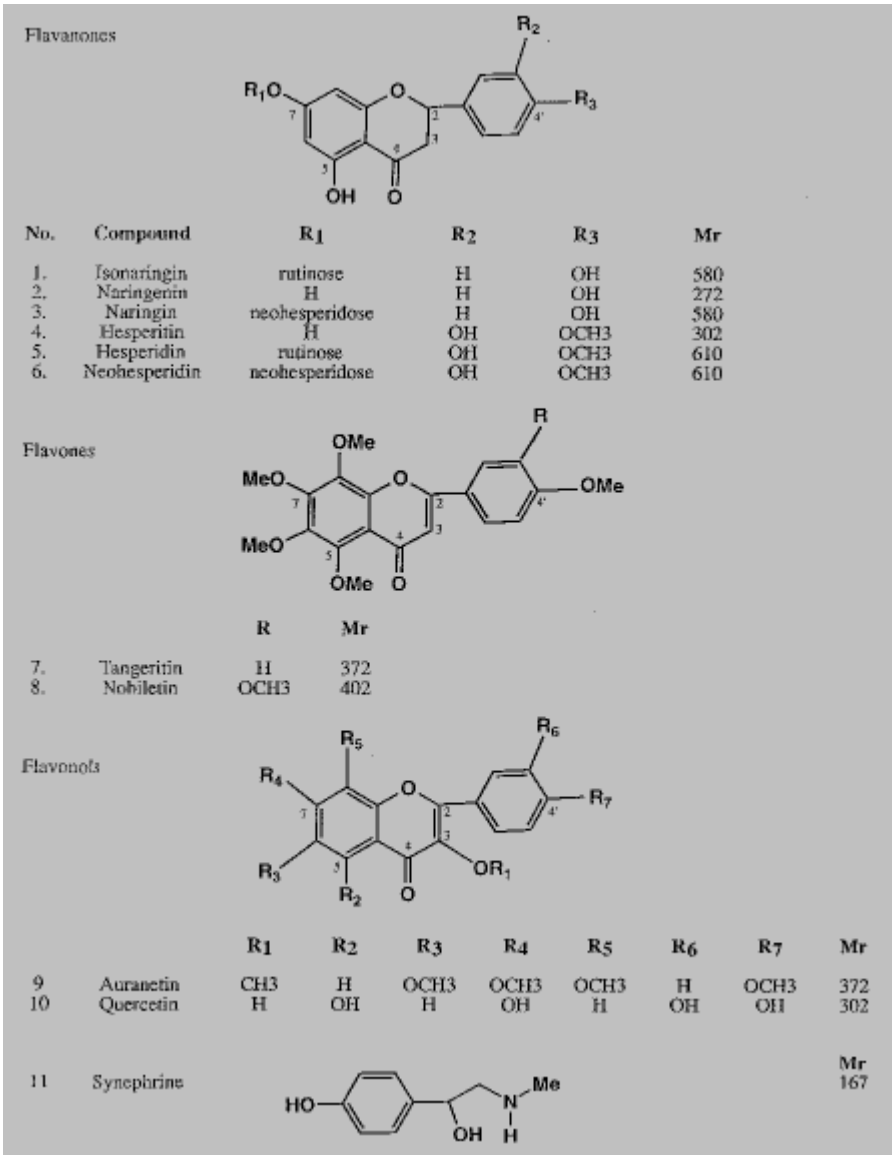

Figure 7. Chemical structures of flavonoids and synephrine found in *Citrus aurantium.* (Ha et al., 1997).

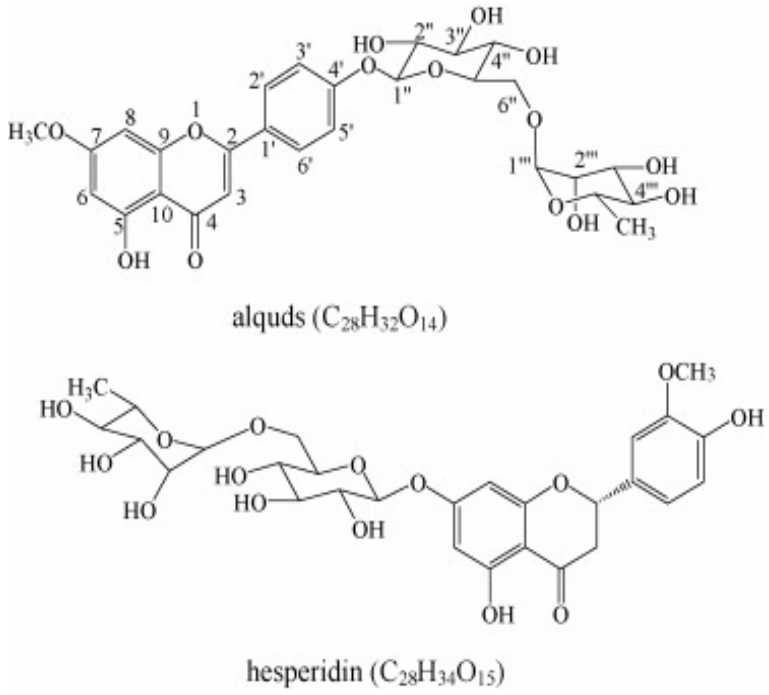

Figure 8. Structure of hesperidin.

2. Materials and Methods

2.1. Materials

Verapamil, norverapamil, hesperidin, and propranolol [an internal standard for the high-performance liquid chromatographic (HPLC) analysis for verapamil and norverapamil] were purchased from Sigma–Aldrich Corporation (St. Louis, MO, USA). Acetonitrile, triethylamine, and diethylether were products from Merck Corporation (Darmstadt, Germany). Phosphoric acid was obtained from Junsei Corporation (Tokyo, Japan). Other chemicals were of reagent grade.

2.2. HPLC analysis

2.2.1. Instrumentation

A high-performance liquid chromatograph (HPLC) equipped with two solvent delivery pumps (Model LC-10AD; Shimadzu Co., Kyoto, Japan), a fluorescence detector (Model RF-10A), a system controller (Model SCL-10A), degasser (Model DGU-12A) and an autoinjector (SIL-10AD).

2.2.2. Chromatographic conditions

The fluorescence detector was set at an excitation wavelength of 280 nm and an emission wavelength of 310 nm. The stationary phase was a Kromasil KR 100-5C_8 column (5 μm; 4.6 mm, i.d.×250 mm, EKA Chemicals, Sweden) and the mobile phase was acetonitrile:0.05 M KH_2PO_4 with 0.05% triethylamine (30:70, v/v; PH 4.0), which was run at a flow rate of 1.5 ml/min. The coefficient of variation for inter- and intra-day was < 12.5%.

2.2.3. Preparation of stock solutions

Stock solutions of verapamil, norverapamil, and propranolol (an internal standard) were prepared by dissolving 10 mg of each drug in 10 ml of methanol. All solutions were stored at –40°C (MDF-292, Sumwon Company, Seoul, South Korea).

2.2.4. Preparation of analytical standard solutions

Each standard solution, verapamil and norverpamil was prepared by diluting the each stock solution with methanol immediately prior to use. All preparations were made in 1.5-ml polyethylene mocrotubes (Axygen Scientific Company, Calif., USA). The standard solutions of verapamil and norverapamil were all 8, 20, 40, 80, 200, 400 and 800 ng/ml. The concentration of propranolol was 2 ng/ml.

2.2.5. Sample preparation

The plasma concentrations of verapamil and norverapamil were determined by a slight modified of an HPLC method reported by Choi et al. (2004). Briefly, a 40-μl aliquot of propranolol HCl (400 ng/ml; an internal standard), a 20-μl aliquiot of 2 N sodium hydroxide solution, and 1.2 ml of diethylether were added to a 0.2-ml aliquot of the plasma sample in a 2.0-ml polypropylene microtube (Axygen Scientific Company, Calif., USA). The mixture was mixed vigorously with a vortex-mixer (Scientific Industries Company, NY, USA) for 2 min and centrifuged (13,000 rpm, 10 min) in a micro centrifuge (Hitachi Company, Tokyo, Japan). A 1.0 ml of the organic layer was transferred into a clean micro tube and evaporated at 35^{o}C under a dry thermo bath (Rikakikai Company, Tokyo, Japan). The residue was dissolved in 200 μl of the mobile phase and centrifuged (13,000 rpm, 5 min). A 50-μl aliquot of the supernatant was directly injected onto the HPLC column.

2.2.6. Validation procedures

2.2.6.1. Linearity

Standard calibration curves were constructed by adding a 50-μl aliquot of verapamil and norverapamil standard solutions at the concentrations of 8, 20, 40, 80, 200, 400 and 800 ng/ml, and a 50-μl aliquot of propranolol at a concentration of 2 ng/ml into a 0.2-ml aliquot each rat blank plasma. Thus, the plasma calibrations were 2, 5, 10, 20, 50, 100 and 200 ng/ml for verapamil plus norverapamil. Then, the extraction procedure was followed as described above. Calibration curves of verapamil and norverapamil were constructed

using the ratio of the peak area of verapamil or norverapamil with that of propranolol. The linearity was determined by construction of a regression line using the method of least sum of squares.

2.2.6.2. Recovery

To determine the extraction efficiency, a 50-µl aliquot of the standard solutions of verapamil and norverapamil at the concentrations of 5, 20 and 100 ng/ml were added separately to a 0.2-ml aliquot of blank plasma samples to yield concentrations of 5, 20 and 100 ng/ml of verapamil and norverapamil in plasma, respectively. Each of these spiked blank plasma samples were treated as those in the sample preparation. The absolute recovery was calculated by comparing the peak areas in 50% of methanol in deionized water (n = 5).

2.2.6.3. Intra- and inter-day variability and determination of LOD and LLOQ

Intra-day variability was obtained from five different rat's plasma samples using the same calibration curve in a day. Inter-day variability was obtained on five different days. The mean relative standard deviation (RSD) of the mean predicted concentration for the independently assayed standards provided the measure of precision. Accuracy was calculated by the percentage deviation of the mean predicted concentration of verapamil and norverapamil from the expected target value.

The limit of detection (LOD) was determined by greater than 3.0 for signal to noise (S/N) ratios. The lower limit of quantification (LLOQ) was determined by spiking a 0.2-ml aliquot of blank rat's plasma with verpamil and norverapamil at the concentration of the lowest calibrator with a precision of 20% and accuracy of ± 20%. The LOD and LLOQ were measured on five different days.

The predetermined criteria for acceptance of both intra- and inter-day results were that the standard concentrations of verapamil and norverapamil had to be accurate within ± 15% of their nominal values as determined by the best-fit regression line except for the LLOQ, where ± 20% was acceptable. The correlation coefficient (r^2) also had to be 0.95 or greater.

2.3. Animal experiments

The protocol of this animal study was approved by the Animal Care Committee of Chosun University, Gwangju, South Korea. Male Sprague–Dawley rats, 7–8 weeks old and weighing 270–300 g, were purchased from the Dae Han Laboratory Animal Research Company (EumSung, South Korea) and given free access to a commercial rat chow diet (No. 322-7-1; Superfeed Company, Gangwon, South Korea) and tap water. They were maintained in a clean room (College of Pharmacy, Chosun University) at a temperature of 22 ± 2 °C with a 12-h light/dark cycle and relative humidity of 50–60%. The rats were acclimated under these conditions for at least 1 week.

2.4. Drug administration and sampe collection

2.4.1. Intravenous (i.v.) administration of verapamil

Each rat was fasted for at least 24 h prior to beginning the experiment. The left femoral artery (for blood sampling) and the left femoral vein (for drug administration in the intravenous study) were cannulated using a polyethylene tube (SP45; i.d., 0.58 mm, o.d., 0.96 mm; Natsume Seisakusho Company, Tokyo, Japan) while each rat was under light ether anesthesia. Verapamil injectable (diluted in 0.9% NaCl-injectable solution) at a dose of 3.0 mg/kg was injected (total injection volume of 1.5 ml/kg) over 0.5 min via the femoral vein. A blood sample (0.45 ml) was collected via the femoral artery into heparinized tubes at 0 (control), 0.017 (at the end of the infusion), 0.1, 0.25, 0.5, 1, 2, 3, 4, 8, 12 and 24 h after the injection. A blood sample was centrifuged (13,000 rpm, 5 min), and a 200-μl aliquot of plasma samples were stored at –40˚C until using for the HPLC analysis of verapamil and norverapamil. A 0.4-ml aliquot of 0.9% NaCl-injectable solution was injected through the femoral vein.

2.4.2. Oral administration of verapamil

Rats were divided into five groups (n = 6, each); oral groups [9 mg/kg of verapamil dissolved in water (3.0 ml/kg)] without (control) or with 3 or 15 mg/kg of hesperidin (mixed in distilled water; total oral volume of 3.0 ml/kg), and an intravenous group (3 mg/kg of verapamil; the same solution used 0.9% NaCl injectable solution; total injection

volume of 1.5 ml/kg). A feeding tube was used to administer verapamil and hesperidin intra-gastrically. Hesperidin was administered 30 min prior to oral administration of verapamil. A blood sample (0.45 ml aliquot) was collected into heparinized tubes via the femoral artery at 0, 0.1, 0.25, 0.5, 1, 2, 3, 4, 8, 12 and 24 h for the oral study. Whole blood (approximately 1 ml) collected from untreated rats was infused via the femoral artery at 0.25, 1, 3 and 8 h, respectively, to replace blood loss due to blood sampling. The blood samples were centrifuged (13,000 rpm, 5 min), and a 200-μl aliquot of plasma samples was stored at –40 °C until the HPLC analysis.

2.5. Pharmacokinetic analysis

Plasma concentration data were analyzed by non-compartmental methods using WinNonlin software version 4.1 (Pharsight Corporation, Mountain View, CA, USA). The elimination rate constant (K_{el}) was calculated by the log-linear regression of diltiazem concentration data during the elimination phase and the terminal half-life ($t_{1/2}$) was calculated as $0.693/K_{el}$. The peak concentration (C_{max}) of diltiazem in plasma and the time to reach C_{max} (t_{max}) were obtained by visual inspection of the data from the concentration–time curve. The area under the plasma concentration–time curve (AUC) from time zero to the time of last measured concentration (C_{last}) was calculated by the linear trapezoidal rule. The AUC zero to infinity ($AUC_{0-\infty}$) was obtained by adding AUC_{0-t} and the extrapolated area determined by C_{last}/K_{el}. The total body clearances of oral (CL/F) diltiazem were calculated from the quotient of the dose (D) and the $AUC_{0-\infty}$ of the intravenous and oral routes. The extent of absolute oral bioavailability (F) was calculated by $AUC_{0-\infty}$ after oral administration by $AUC_{0-\infty}$ afrer intravenous administration. The relative bioavailability (R.B.) of verapamil was calculated by $AUC_{\text{verapamil with}}/AUC_{\text{verapamil without}}$. The metabolite–parent ratio (M.R.) was calculated by $AUC_{\text{norverapamil}}/AUC_{\text{verapamil}}$.

2.6. Statistical analysis

The pharmacokinetic parameters were compared using a one-way ANOVA, followed by a posteriori testing with the Dunnett correction. Differences were considered significant at

a level of $p < 0.05$. All data are expressed in terms of mean ± S.D.

3. Results and Discussion

Figure 9 depicts the chromatograms of blank rat plasma sample (A), plasma sample

collected (0.5 hour) after oral administration of verapamil (B) to rats. The retention times of propranolol (an internal standard, IS), verapamil, and norverapamil were 4.7, 16, and 13.9 min, respectively. The overall run time lasted 18 min.

Calibration curves for verapamil (Figure 10) and norverapamil (Figure 11) constructed by plotting the ratio of the peak area of verapamil or norverpamil to that of propranolol as a function of the plasma verapamil or norverapamil concentrations (2, 5, 10, 20, 50, 100 and 200 ng/ml). There is a good linearity over the range of 2–200 ng/ml with a mean correlation coefficient of 0.997 (verapamil) and 0.998 (norverapamil). The typical equation describing the calibration curve in rat's plasma was $y = 0.0232\ x + 0.1297$ (for verpamil) and $y = 0.0195\ x - 0.0663$ (for norverpamil), where y is the peak area ratio of verapamil or norverpamil to propranolol and x is the concentration of verapamil or norverpamil, respectively.

The recovery of verpamil or norverapamil after liquid-liquid extraction procedure was evaluated at three concentrations (5, 20 and 100 ng/ml, respectively). The recovery of the verapamil and norverapamil was above 84.3–88.0% and 82.6–83.9%, respectively, when spiked concentration in rat plasma was 2.0 ng/ml (Table 1).

The LOD for verapamil or norverapamil in rat plasma defined as a s/n ratio of greater than 3 was 2 ng/ml. The LLOQ for verapamil (Table 2) was 2 ng/ml with an acceptable precision and accuracy (RSD: 12.6%, deviation: −8.5%, n = 5). The LLOQ for norverapamil (Table 3) was 2 ng/ml with an acceptable precision and accuracy (RSD: 13.1%, deviation: −10%, n = 5).

Figure 12 depicts the mean plasma concentration–time profiles of verapamil after oral administration (9 mg/kg) with or without of hesperidin (3 or 15 mg/kg), and Table 6 lists the pharmacokinetic parameters of verapamil after oral administration. Hesperidin significantly ($p < 0.01$) increased the area under the plasma concentration–time curve (AUC) and the peak concentration (C_{max}) of verapamil by 71.1–96.8% and 98.3–105.2%, respectively, and hesperidin increased the terminal half-life ($t_{1/2}$) of verapamil but not significantly. Hesperidin significantly ($p < 0.01$) decreased the total plasma clearance (CL/F) of verapamil by 41.6–49.2%. Consequently, compared with the control group (4.6%), the absolute oral bioavailability (F) of verapamil with hesperidin was increased significantly by 7.9–9.0%, and the relative bioavailability (R.B.) of verapamil was

increased by 1.71– to 1.96–fold than those of the control group. It has been reported that human gut wall CYP3A4 is inhibited by grapefruit juice (containing hesperidin) (Fuhr et al., 2002), and bioflavonoid such as hesperidin, an inhibitor of P-gp, significantly increased the permeation of vincristin across the blood-brain barrier (Yoshiharu et al., 2000). The enhanced F of verapamil by hesperidin might be due to inhibition of CYP3A4 and P-gp in the intestine and liver. This result appeared to be consistent with previous studies reported by Kim et al. (2005); a single oral administration of flavonoid, naringin (7.5 mg/kg) significantly increased the AUC and C_{max} of verapamil in rabbits, which was due to inhibition of CYP3A4 and P-gp. Hesperidin did not affect the K_{el} and T_{max} of verapamil.

Figgure 13 depicts the mean plasma concentration–time profiles of norverapamil after oral administration of verapamil (9 mg/kg) with or without hesperidin (3 or 15 mg/kg). As listed in Table 7, hesperidin significantly ($p < 0.05$) increased the AUC of norverapamil by 67.7–79.3% and the C_{max} by 60.5–64.7%. Hesperidin increased the $t_{1/2}$ of norverapamil but not significantly different form the control group. Norverapamil and D-617 are substrate and inhibitor of P-gp (Pauli-Magnus et al., 2000; Woodland et al., 2003). These results suggest the metabolism and/or absolution verapamil may be inhibited by hesperidin. Therefore, the enhanced $AUC_{norverpamil}/AUC_{verpamil}$ might be due to inhibition of CYP3A4 by hesperidin in the intestine and liver (Tai and Liu, 2004). Hesperidin did not affect the K_{el} and T_{max} of norverapamil. However, the metabolite-parent ratio (M.R.) of norverapamil by hesperidin decreased but is not significant compared to that of the control group, implying that presence of hesperidin could be effective to inhibit the CYP3A-mediated metabolism of verapamil.

There is a growing body of evidence that CYPs in enterocytes contribute significantly to the “first-pass” metabolism and oral bioavailability of many drugs and chemicals. The “first pass” metabolism of compounds in the intestine and liver reduces F, limits absorption of toxic xenobiotics and may ameliorate adverse effects. Moreover, induction or inhibition of intestinal CYPs may be responsible for significant drug/drug interactions when one agent decreases or increases the F and K_a of biotransformation of a concurrently administered drug (Kaminsky and Fasco, 1991).

Orally administered drugs must pass through the small intestinal membrane to access the

systemic circulation (Figure 3). Like other lipophilic drugs, most of verapamil is absorbed via the apical enterocytes of the villi of small intestine where full of CYP3A and P-gp rather than via the deep crypts with low level of CYP3A and P-gp or the splanchnic capillaries by paracellular transport, which attribute to the considerable exposure of verapamil in CYP3A and P-gp of the enterocyte (Figure 3). Second, although the protein binding is not correlated with the exposure in the enterocytes, it is of magnitude for the exposure in the hepatocytes because only free form can pass through the sinusoidal membrane of hepatocytes. The high level protein binding of verapamil (90%) should be one of the contributors to its low hepatic first-pass effect (Schomerus et al., 1976). Last, the blood flow rate in the liver is 55.2 ml/min/kg in rats, and in the value the gut is 30 ml/min/kg (Davies and Morris, 1993). Thus, the blood flow rate in the small intestine is considerably lower than that in the liver. The slower of blood flow rate would increase residence time of verapami in the intestine during first-pass compared to hepatocyte, which can be another contributor to the high intestinal first-pass extraction of verapamil than the liver. Choi and Han (2004) reported that quercetin, a dual inhibitor of CYP3A and P-gp, significantly enhanced the F of verapamil in rats. The factors within the gastrointestinal tract such as transporter mediated intestinal secretion, or gut wall metabolism may contribute considerably to the variable oral F of verapamil.

The involvement of P-gp in risperidone disposition has recently been documented (Boulton et al., 2002, Wang et al., 2004 and Nakagami et al., 2005). In the intestine, P-gp is expressed on the brush-border membrane of enterocytes and pumps compounds out of cells from the cytosol to the intestinal lumen. P-gp has been labelled a transport barrier to the oral absorption of drugs (Leu and Huang, 1995, Fricker et al., 1996, Lown et al., 1997, Kim et al., 1998 and Salphati and Benet, 1998). Moreover, P-gp could act along with CYP3A4 to increase drug presystemic metabolism (Gan et al., 1996, Watkins, 1997, Wacher et al., 1998 and Ito et al., 1999). The above mentioned two mechanisms have been proposed to explain how P-gp may enhance the extent of intestinal absorption. According to a first mechanism, P-gp activity induces repeated cycles of secretion of drug into the intestinal lumen, resulting in repeated cycles of absorption. The residence time of a drug in the intestine and its exposure to intestinal CYP3A4 are lengthened prior to systemic absorption (Gan et al., 1996). A second mechanism has been proposed suggesting that P-

gp may facilitate the removal of intracellular primary metabolites, thus minimising the potential to produce CYP3A4 inhibition (Lown et al., 1997).

The increased bioavailability of verapamil by hesperidin suggests that CYP3A and P-gp could be inhibited by hesperidin, which resulted in reducing first-pass metabolism of verapamil. In the above mentioned results were consistent with the results reported by Choi et al. (2004), in that flavonoid (quercetin) significantly enhanced the oral bioavailability of verapamil in rabbits (Choi and Han, 2004). And similar to our previous study (Choi and Han 2005), morin inhibited P-gp and CYP3A, enhanced absorption of verapamil in rats.

Table 1. Recovery of verapamil and norverapamil from rat plasma

Concentration (ng/ml)	Peak area (mean ± S.D., n = 5)	Recovery (%)

	Extracted	Unextracted	
Verapamil			
5	6730 ± 128.9	5673 ± 1120.5	84.3
20	32652 ± 6528.2	27656 ± 5431.6	84.7
100	115348 ± 22989.2	101506 ± 20191.3	88.0
Norverapamil			
5	5031 ± 998.8	4156 ± 826.5	82.6
20	20144 ± 4013.6	16941 ± 3369.9	84.1
100	98566 ± 19613.2	82697 ± 16486.5	83.9

Table 2. Precision and accuracy of HPLC assay for verapamil from rat plasma

Spiked concentration (ng/ml)	Calculated concentration (ng/ml, mean ± S.D., n = 5)	RSD (%)	Deviation (%)

Intra-day (n = 5)			
2	1.83 ± 0.23	12.6	–8.5
5	4.88 ± 0.50	10.2	–2.4
10	9.91 ± 0.91	9.2	–0.9
20	19.5 ± 1.52	7.8	–2.5
50	49.7 ± 2.14	4.3	–0.6
100	99.8 ± 3.79	3.8	–0.2
200	201 ± 3.22	1.6	0.5
Inter-day (n = 5)			
2	1.80 ± 0.24	13.1	–10.0
5	4.92 ± 0.63	12.8	–1.6
10	9.88 ± 1.0	10.1	–0.2
20	20.5 ± 1.97	9.6	2.5
50	48.9 ± 3.81	7.8	–2.2
100	99.2 ± 4.96	5.0	0.8
200	199.6 ± 6.39	3.2	–0.2

Table 3. Precision and accuracy of HPLC assay for norverapamil from rat plasma

Spiked concentration (ng/ml)	Calculated concentration (ng/ml, mean ± S.D., n = 5)	RSD (%)	Deviation (%)

Intra-day (n = 5)			
2	1.80 ± 0.23	13.1	–10.0
5	4.79 ± 0.53	11.1	–4.2
10	9.90 ± 1.04	10.5	–1.0
20	19.3 ± 1.58	8.2	–3.5
50	49.8 ± 2.29	4.6	–0.4
100	99.4 ± 3.48	3.5	–0.6
200	198.3 ± 3.56	1.8	–0.9
Inter-day (n = 5)			
2	1.79 ± 0.24	13.2	–10.5
5	4.67 ± 0.50	10.8	–6.6
10	9.81 ± 0.99	10.1	–1.9
20	19.1 ± 1.62	8.5	–4.5
50	49.3 ± 2.61	5.3	–1.4
100	99.1 ± 3.36	3.4	–0.9
200	199.0 ± 3.98	2.0	–0.5

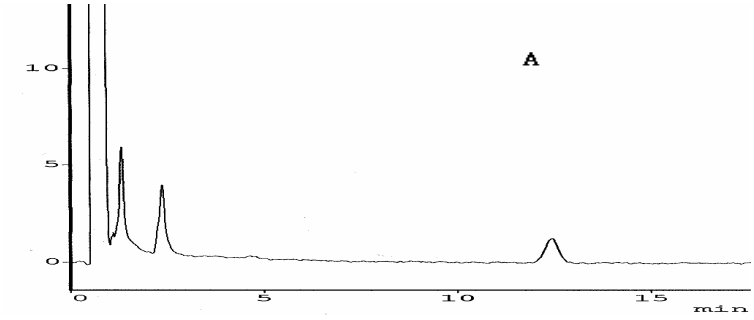

Figure 9. Chromatograms of rat blank plasma (A) and plasma (B) spiked with norverapamil (13.9 min), verapamil (16.0 min), and an internal standard, propranolol (4.7 min).

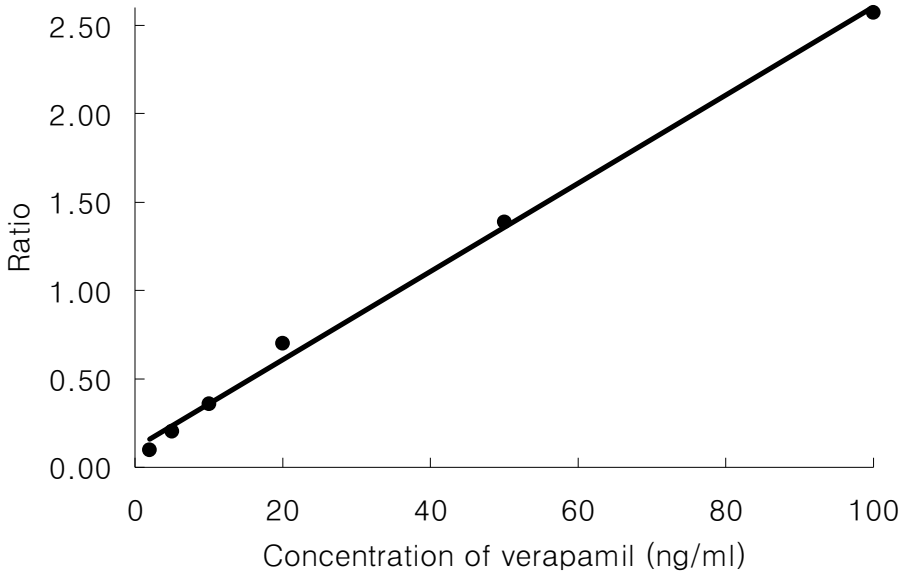

Figure 10. A calibration curve for verapamil when spiked into rat blank plasma, where *y* is the peak area ratio of verapamil against propranolol and *x* is the concentration of verapamil. $y = 0.0232\ x + 0.1297$ ($R^2 = 0.997$).

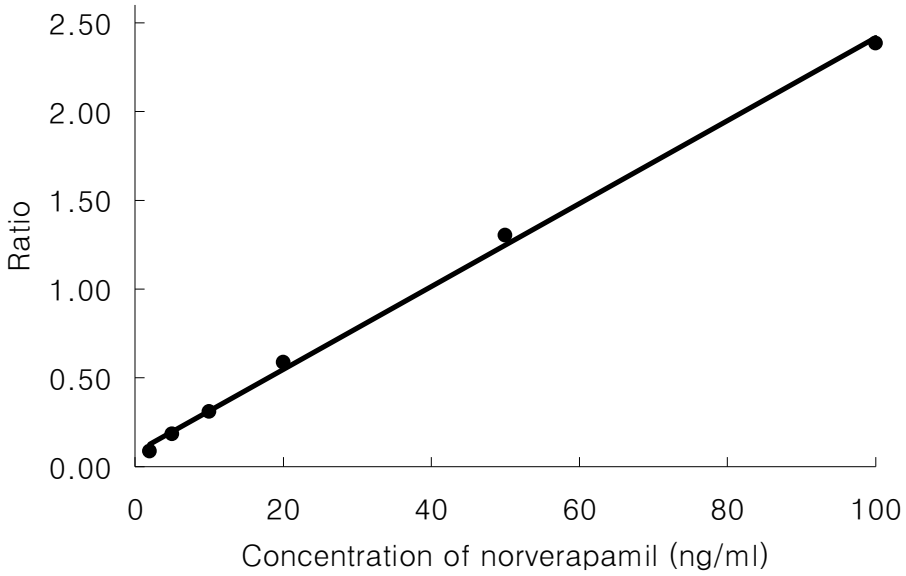

Figure 11. A calibration curve for norverapamil when spiked into rat blank plasma, where *y* is the peak area ratio of norverapamil against propranolol and *x* is the concentration of norverapamil. $y = 0.0195\,x - 0.0663$ ($R^2 = 0.998$).

Table 4. Mean (± S.D.) plasma concentrations of verpamil after its intravenous or oral administration at a dose of 9 mg/kg with or without of hesperidin at a dose of 3 or 15 mg/kg in rats (n = 6, each).

Time (h)	Control (oral)	Verapamil + Hesperidin		Verapamil (i.v.)
		3 mg/kg	15 mg/kg	
0.0	0	0	0	4836 ± 62.1
0.1	35 ± 8.4	63 ± 15.4	61 ± 15.1	1432 ± 62.1
0.25	58 ± 14	106 ± 26.3	112 ± 26.7	1025 ± 87.5
0.5	56 ± 13.8	115 ± 28.7	119 ± 28.1	676 ± 90.6
1	36 ± 8.6	63 ± 15.3	64 ± 15.2	367 ± 78.4
2	24 ± 6.0	34 ± 8.4	35 ± 8.4	158 ± 74.4
3	17 ± 4.1	22 ± 5.5	24 ± 5.8	88 ± 58.3
4	11 ± 2.4	16 ± 3.8	19 ± 4.3	45 ± 15.3
8	7.2 ± 1.7	12 ± 2.8	13 ± 3.4	16.1 ± 11.9
12	5.0 ± 1.2	9.2 ± 2.1	10 ± 2.3	7.2 ± 8.06
24	2.6 ± 0.63	5.1 ± 1.1	6.0 ± 1.3	2.5 ± 6.27

Table 5. Mean (± S.D.) plasma concentrations of norverapamil after oral administration of verapamil at a dose of 9 mg/kg with or without hesperidin at a dose of 3 or 15 mg/kg to rats (n = 6, each).

Time (h)	Control	Verapamil + Hesperidin	
		3 mg/kg	15 mg/kg
0	0	0	0
0.1	12.3 ± 2.92	16.2 ± 4.01	16.9 ± 4.21
0.25	29.4 ± 7.21	38.1 ± 9.11	40.2 ± 9.89
0.5	37.1 ± 9.05	60.2 ± 14.2	61.8 ± 15.2
1	38.0 ± 9.41	61 ± 14.8	62.6 ± 15.4
2	23.7 ± 5.81	37.6 ± 9.21	39.4 ± 9.87
3	16.5 ± 4.02	26.4 ± 6.38	27.8 ± 6.89
4	11.9 ± 2.76	17.2 ± 4.28	18.7 ± 4.59
8	7.8 ± 1.84	12.5 ± 3.14	13.8 ± 331
12	5.4 ± 1.15	8.5 ± 2.01	9.2 ± 2.15
24	2.8 ± 0.69	5.2 ± 1.10	5.9 ± 1.29

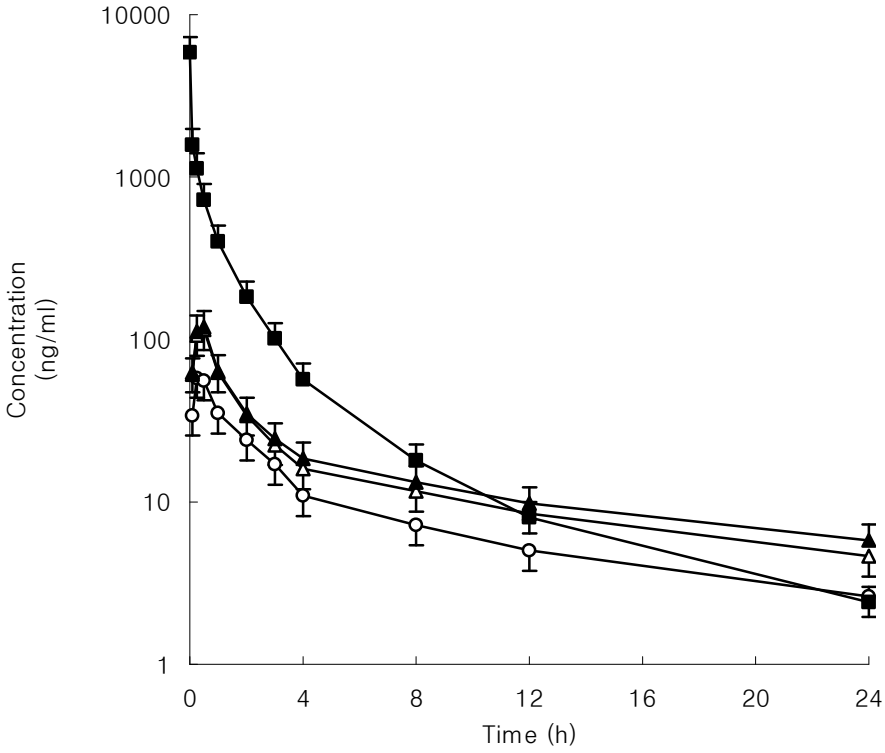

Figure 12. Mean plasma concentration–time profiles of verapamil following intravenous (3 mg/kg) or oral (9 mg/kg) administration of verapamil to rats with or without hesperidin (Mean ± S.D. n = 6). (○) Control (verapamil 9 mg/kg, oral); (△) the presence of 3 mg/kg of hesperidin; (▲) the presence of 15 mg/kg of hesperidin; (■) i.v. injection of verapamil 3 mg/kg. Bars represent the standard deviation.

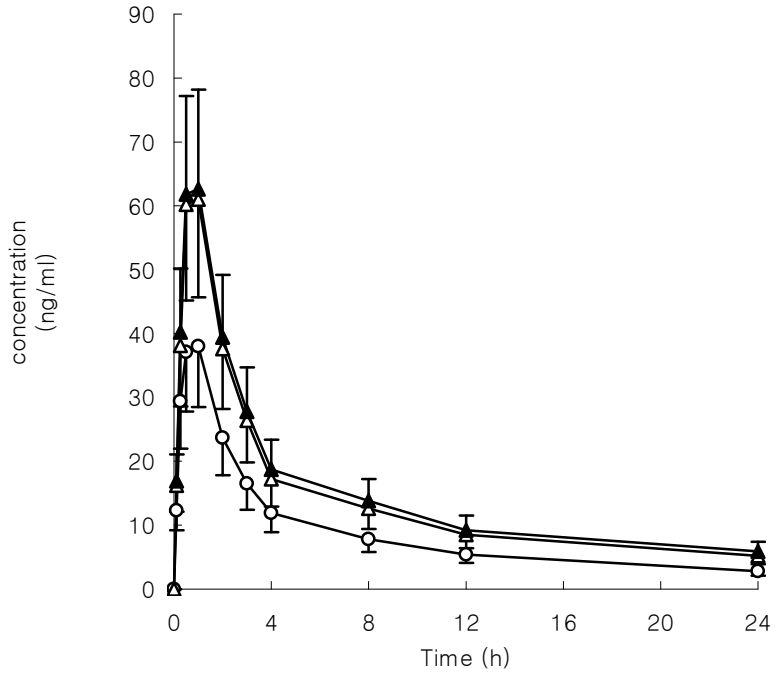

Figure 13. Mean plasma concentration–time profiles of norverapamil after oral administration of verapamil (9 mg/kg) to rats with or without hesperidin (Mean ± S.D., n = 6). (○) Control (verapamil 9 mg/kg, oral), (△) the presence of 3 mg/kg of hesperidin, (▲) the presence of 15 mg/kg of hesperidin. Bars represent the standard deviation.

Table 6. Mean (± S.D.) pharmacokinetic parameters of verapamil after intravenous (3 mg/kg) or oral administration of verapamil at a dose of 9 mg/kg with or withut hesperidin at a dose of 3 or 15 mg/kg to rats (n = 6, each).

Parameter	Control (oral)	Verapamil + Hesperidin		Verapamil (i.v.)
		3 mg/kg	15 mg/kg	
AUC (ng·h/ml)	257 ± 58	433 ± 108**	498 ± 124**	1667 ± 403
C_{max} (ng/ml)	58 ± 14	115 ± 28.9**	119 ± 30**	-
T_{max} (h)	0.25	0.5	0.5	-
CL/F	583 ± 150	346 ± 86**	301 ± 71**	-
K_{el} (h)	0.068 ± 0.016	0.061 ± 0.016	0.056 ± 0.014	0.139 ± 0.031
$t_{1/2}$ (h)	10.0 ± 2.4	11.4 ± 2.9	12.4 ± 3.0	5.1 ± 1.12
F (%)	5.15	7.9	9.0	-
RB (%)	100	171	196	-

**p < 0.01; compared to control.

AUC: area under the plasma concentration–time curve from 0 to 24 h

C_{max}: peak concentration

CL/F: total plasma clearence

K_{el}: elimination rate constant

$t_{1/2}$: terminal half-life

T_{max}: time to reach peak concentration

F: absolute oral bioavailability

RB: relative bioavailability

Table 7. Mean (± S.D.) pharmacokinetic parameters of norverapamil after oral administration of verapamil at a dose of 9 mg/kg with or without hesperidin at a dose of 3

or 15 mg/kg to rats (n = 6, each).

Parameter	Control	Verapamil + Hesperidin	
		3 mg/kg	15 mg/kg
AUC (ng·h/ml)	251 ± 64	423 ± 106*	455 ± 110*
C_{max} (ng/ml)	38.0 ± 9.5	61.0 ± 14.8*	62.6 ± 15.9*
T_{max} (h)	1.0	1.0	1.0
$t_{1/2}$ (h)	9.91 ± 2.5	11.8 ± 3.1	11.9 ± 3.1
K_{el} (h)	0.070 ± 0.018	0.059 ± 0.015	0.058 ± 0.015
MR	0.98 ± 0.25	0.95 ± 0.24	0.89 ± 0.22
RB (%)	100	169	181

*$p < 0.05$; compared to control.

AUC: area under the plasma concentration–time curve from 0 to 24 h

C_{max}: peak concentration

K_{el}: elimination rate constant

$t_{1/2}$: terminal half-life

T_{max}: time to reach peak concentration

RB: relative bioavailability

MR: Metbolite Parent ratio

4. Conclusion

A flavonoid, hesperidin, enhanced the F of verapamil. Because hesperidin have many health-promoting benefits and have no consistent side effects, it might be available as the MDR modulators in the clinical therapy to improve the oral F of verapamil in humans.

Part Ⅱ Effects of Epigallocatechin gallate on the Oral Bioavailability of Verapamil in Rats

Abstract

Favonoids can modulate the P-glycoprotein (P-gp) and cytochrome P450 (CYP) 3A. The F of many drugs are low which contirbute highly to the first-pass efffect caused mainly by phase 1 and phase 2 metabolism, and the members of ATP-binding cassettte (ABC) superfamily mediated efflux by p-gp in the intestine and the liver. Thus this study investigated the pharmacokinetics of intravenous or oral administration of verapamil in rats in order to examine the effects of CYP3A and/or P-gp by hesperidin on the oral bioavailability of verapamil and one of its metabolites, norverapamil. Epigallocatechin gallate (EGCG), flavonoid, are suggested to inhibit P-gp and CYP3A *in vitro*. A single oral (9 mg/kg) dose of verapamil was administered to rats with or without oral administration of EGCG at a dose of 3 or 15 mg/kg, respectively, was oral administered 30 min prior to the oral administration of verapamil, respectively. Plasma concentrations of verapamil and norverapamil well determined using an HPLC analysis with a fluorescence detector.

Compared to the oral control group, EGCG significantly ($p < 0.01$) increased the AUC of verapamil by 85.2–127% and the C_{max} by 102–136%, and the presence of EGCG was increased the $t_{1/2}$ of norverapamil but not significantly. EGCG significantly ($p < 0.01$) decreased the CL/F of verapamil by 46.0–55.9%. There was no significant change in the T_{max} and K_{el} of verapamil by EGCG.

Compared to the oral control group, EGCG significantly ($p < 0.05$) increased the AUC of norverapamil by 72.9–93.9% and the C_{max} by 65.3–72.9%, and the presence of EGCG was increased the $t_{1/2}$ of norverapamil but is not significantly. The metabolite-parent ratio (M.R.) of norverapamil with EGCG decreased but is not significantly. There was no significant change in the time to reach the peak plasma concentration (T_{max}) and the elimination rate constant (K_{el}) of norverapamil with EGCG.

The enhanced F of verapamil was observed combination by natural flavonoid, EGCG. It is possible that these natural flovonoids could act as modulators of P-gp and/or CYP3A to improve the F of verapamil in humans. The pharmacokinetic interaction between

verapamil and EGCG should be taken into consideration in the clinical setting.

Key words: Verapamil, Norverapamil, Epigallocatechin gallate (EGCG), Pharmacokinetics, Bioavailability, P-gp, CYP3A, Rats.

1. Introduction

The microsomal cytochrome P450 isoenzymes (CYPs) comprise a large group of hemoproteins with monooxygenase activity. They play a major role in the metabolism of numerous xenobiotics, including drugs, carcinogens, pesticides, hydrocarbons, and endogenous compounds, such as steroids. These enzymes are located in various tissues (liver, brain, gut, kidney, and lung) in which several isoenzymes may be expressed simultaneously (Gushchin et al., 1999).

The CYP3A subfamily is the most important to drug metabolism in humans, because they metabolize the majority of commercially available drugs (Wrighton et al., 2000). There are four differentially regulated CYP3A genes in humans, CYP3A4, CYP3A5, CYP3A7 and CYP3A43. CYP3A4 is generally thought to be the predominant form expressed in the liver cells (Wrighton et al., 2000). Recently, it has become apparent that the kinetic interaction between CYP enzymes and their substrates *in vitro* is often atypical, as exemplified by CYP3A4 (Figure 1).

The transport-based classical multi-grug resistance (MDR) is caused by the ATP-binding cassette (ABC) family, a membrane transport ATPases. The general structures of ABC transporters compose of 12 transmembrane (TM) regions, split into two ‘halves’, each with a nucleotide-binding domain (NBD) (Figure 2A), such as P-gp (MDR1), MDR3, BSEP (SP-gp), multidrug resistance-associated protein (MRP) 4, MRP5, and MRP8. The MRP1–3 and MRP6–7 have an additional five TM regions at the N-terminus (Figure 2B). Breast cancer-resistance protein (BCRP) has only six TM regions and one NBD (Figure 2C), which was proposed to function as a dimer (Ozvegy et al., 2001). NDBs play a role in cleaving ATP (hydrolysis) to derive energy necessary for transporting cell nutrients, such as sugars, amino acids, ions and small peptides across membranes.

Althought the overall model of 12 transmembranere regions has been generally well-supported by antibody localization data (Yoshimura et al., 1989), an alternative model has recently appeared based on the coupled *in vitro* translation and translocation of P-gp into dog pancreas microsome membranes (Zhang et al., 1991). This study suggests, based on the presence of a glycosylated segment in the carboxy-terminal half of P-gp, that under some conditions in mouse P-gp, the eighth and ninth transmembrane domains, and the amino acids between transmembraned omains 8 and 9, might be extracellular rather than cytoplasmic as suggested in the model shown in Figure 2. These results are supported by

in vivo expression of truncated P-gp chimeras in *Xenopuso* ocytes, as well as by *in vitro* expression of intact human P-gp in a cell-free translation-translocation system (Skach et al., 1993). Howevers, study proteolytic fragments of photoaffinity-labelled P-gp indicates that there does not appear to be a glycosylated region in the carboxy-terminal half of mature human P-gp, arguing against this model of 10 transmembrane regions for a form of P-gp capable of binding drugs (Bruggemann et al., 1989, 1992). However, it is possible that this region is indeed extracellular, but not glycosylated or that P-gp with this variant topology does not survive to the cell surface because of intracellular degradation. The precise topology of P-gp on the mammaliacne ll surface needs further study.

Since the original publication of the human MDR1 and mousem dr3 (mdrla) sequences, full-length sequences have appeared for mouse mdrlb (also called mdr2) (Devault et al., 1990)), mousem dr2 (Gros et al., 1988), human MDR2 (Van der Bliek et al., 1988), hamster p-gpl (similar to mdrla) (Devine et al., 1991), and the rat mdrlb gene (Silverman et al., 1991). Comparison of these sequences shows a considerable amount of sequence identity and homology among mdr family members (Devine et al., 1991). For example, the human MDRI and MDR2 coding sequences are 76% identical despite different abilities to transport drugs, and the mouse mdrla and human MDR1s equences, with similar function, are 88%i dentical, despite 50 million years or moreo fevolution. Amongth e mdr genes that function as multidrug transporters, the regions of greatest homology are the ATP-binding/utilizationr egions, and the first and secondi ntracytoplasmic loops in each half of the molecule. The least conserved regions are the first extracytoplasmic loop, where even glycosylation sites are not preserved, the intracellular linker region.

P-gp is also present at the normal tissues such as kidney and adrenal gland (high level), liver, small intestine, colon and lung (medium level), and prostate, skin, spleen, heart, skeletal muscle, stomach and ovary (low level) (Fojo et al., 1987; Gatmaitan and Arias, 1993). Same as P-gp, MRP1 is highly expressed in intestine, kidney, lung and lower in liver (Cherrington et al., 2002; Flens et al., 1996; Zaman et al., 1993) and MRP2 is expressed mainly in liver, intestine, and kidney tubules (Fromm et al., 2000; Schaub et al., 1997). As shown in Figure 3, P-gp and MRPs spreaded in the excretory organs provide a barrier to eliminate the substrates out of the body. P-gp and MRP2 co-localized to the apical membrane of the intestine, liver, kidney, and blood-brain barrier (Thiebaut et al.,

1987; Buchler et al., 1996; Fromm et al., 2000; Schaub et al., 1999), and MRP1 is localized to the basolateral membranes of polarized epithelial cells of the intestinal crypt (Peng et al., 1999), renal distal and collecting tubules (Peng et al., 1999), and liver (Mayer et al., 1995; Roelofsen et al., 1997).

P-gp and MRPs are reportedly co-localized with phase I and phase II metabolizing enzymes, CYP3A4, UDP-glucuronosyltransferases, and glutathione-*S*-transferases in the liver, kidney and intestine (Sutherland et al., 1993; Turgeon et al., 2001) (Figure 3). The CYP3A subfamily involves in approximately 40–50% of phase I metabolism of marketing drugs (Guengerich, 1995). Specifically, CYP3A4 accounts for 30% of hepatic CYP and 70% of small intestinal CYP (Schuetz et al., 1996). A substantial overlap in substrate specificity exists between CYP3A4 and P-gp (Wacher et al., 1995). Additionally, the phase II conjugating enzymes, such as UDP-glucuronosyltransferases and glutathione-*S*-transferases, may subsequently modify either the phase I metabolites or the parent compounds as the conjugated compounds, and further subject toMRP2-mediated efflux in the liver and intestine. Thus, a synergistic relationship exists between the transporters and metabolic enzymes, such as CYP3A4 versus P-gp and conjugating enzymes versus MRP2, within excretory tissues to protect the body against invasion by foreign compounds, which also decrease the oral bioavailability of many drugs, especially anticancer drugs.

Oral administration of drugs has many advantages over intravenous injection because it is less invasive, easier to use for the patient in a chronic regimen and more cost-effective because of decreased hospitalization. The small intestine represents the principal site of absorption for orally administered compounds. There are two principal pathways, paracellular and transcellular, in the intestinal epithelium that allows the compounds to cross. Some small hydrophilic, ionized drugs are absorbed via the paracellular pathway for there small particle size is suitable for pass through the tight intercellular junctions (Hayashi et al., 1997). Many orally administered drugs are lipophilic and undergo passive transcellular absorption (Hunter and Hirst, 1997). Drugs that cross the apical membrane or present in the blood would be substrates for apical efflux of transporters, specifically ABC proteins such as P-gp and MRP2, and cytochrome P450 (especially CYP3A4)-mediated Phase I metabolism of orally ingested compounds (Watkins, 1992). Phase I and phase II metabolic enzymes may yield metabolites that are themselves substrates for efflux pumps,

such as P-gp and MRP2 (Keppler et al., 1999). The fraction of compounds that escapes this first barrier will pass to the liver via the portal vein and subject to further metabolism and biliary excretion by the same enzymes and transporters present in the enterocytes, which complete the first cycle of enterohepatic circulation (first-pass extraction). Drugs that reach the systemic circulation following first pass extraction by the liver, or through the lymphatics, will meet the kidneys, which are also well equipped with the efflux transporters for the active excretion of the parent or the metabolites of the compounds. The efflux transporters and intracellular metabolic enzymes in the intestine and liver are critical determinants of overall oral bioavailability.

Verapamil is a calcium channel-blocker that is widely used as an antiarrhythmic agent to control supraventricular tachyarrhythmias. Verapamil is also useful for the treatment of hypertension, ischemic heart disease and hypertrophic cardiomyopathy on account of its potent vasodilating and negative inotropic properties (Fleckenstein, 1977; Gould et al., 1982; Lewis et al., 1978). Treatment with verapamil is generally well tolerated, but adverse effcts connected with verapamil is pharmacological effects on cardiac conduction can arise and may be particularly severe in patients with hypertrophic cardiomyopathies. Adverse effects on the heart include bradycardia, atrioventricular block, worsening heart failure, and transient asystole. These effects are more common with parenteral than with oral therapy. The most troublesome non-cardiac adverse effect is constipation. Nausea may occur but is less frequently reported. Other adverse effects include hypotension, dizziness, flushing, headaches, fatigue, dyspnoea, and peripheral oedema. There have been reports of skin reactions and some cases of dbnormal liver function and hepatotoxicity. Gingval hyperplasia has ocurred. Gynaecomastia has been reported rarely (Fleckenstein, 1977; Gould et al., 1982; Lewis et al., 1978).

Verapamil is approximately 90% absorbed from the gastrointestinal tract, but is subject to very considerable first-pass metabolism in the liver and the bioavailability is only about 20%. Verapamil exhibits bi-or tri-phasic elimination kinetics and is reported to have a terminal plasma half-life of 2 to 8 hours following a single oral dose or after intravenous adnimistration. Verapamil is about 90% bound to plasma proteins (Schomerus et al., 1976). In humans, N-desalkylverapamil (D-617) was the most abundant metabolite in 0-48h urine at a percentage of the excreted dose of 22%, followed by O-desmethyverapamil (D-703;

7%), norverapamil (N-desalkylverapamil; 6%) (Eichelbaum et al., 1979) (Figure 4). Norverapamil is an N-demethylated metabolite of verapamil with approximately 20% of the coronary vasodilating activity of the parent compound in dogs (Eichelbaum et al., 1984). The formation of norverapamil and D-617 was mediated via hepatic microsomal cytochrome P450 (CYP) 3A4 and 1A2, and CYP3A and to a lesser extent, CYP1A2 are the principal mediators of verapamil biotransformation in humans (Levy et al., 2000). Verapamil is a known to be substrate P-gp as well as CYP3A4 (Doppenschmitt et al., 1999; Adachi et al., 2001; Pauli-Magnus et al., 2000; Saitoh and Aungst, 1995). Furthermore, it has been reported that the phase 1 metabolites of verapamil exhibit different P-gp substrate and inhibition characteristics (Hau β ermann et al., 1991; Pauli-Magnus et al., 2000; Woodland et al., 2003). While N-dealkylated metabolites (D-617 and D620) are P-gp substrates, norverapamil and O-demethylated metabolite (D-703) are inhibitors of P-gp function, implying that verapamil metabolites may influence P-gp mediated drug disposition and elimination. P-gp is colocalized with CYP 3A4 at the apical membrane of the cells in the small intestine (Gottesman and Pastan, 1993). Which is a membrane transporter that actively "pumps" xenobiotics out of cells (Doppenschmitt et al., 1999). In the small intestine, P-gp is colocalized with CYP3A4 at the apical membrane of the cells (Gottesman and Pastan, 1993).

Flavonoids are widely distributed in dietary supplements such as vegetables, fruit, tea and wine (Hertog et al., 1993b). Flavonoids have many beneficial effects including antioxidant, antibacterial, antiviral, antiinflammatory, antiallergic, and anticarcinogenic actions (Ross and Kasum, 2002; Hodek et al., 2002) though whether these effects can be attributed to the aglycone forms or their metabolites is not entirely clear. The total daily intake of flavonoids via the dietary supplements has been 23 mg/day in Dutch population (Hertog et al., 1993a), among which the most important flavonoid was the flavonol quercetin (mean intake 16 mg/day). Many flavonoids are ubiquitous in all parts of the plant. Flavonoids are polyphenolic compounds possessing 15 carbon atoms; two benzene rings joined by a linear three-carbon chain (Figure 5A). A chromane ring bearing a second aromatic ring B in position 2, 3 or 4 (Figure 5B). The oxygen bridge involving the central carbon atom (C_2) of the three-carbon chain occurs in a rather limited number of cases, where the resulting heterocyclic is of the furan type. Various subgroups of flavonoids are

classified according to the substitution patterns of ring C. Both the oxidation state of the heterocyclic ring and the position of ring B are important in the classification. The major subgroups of flavonids are as followes (Figure 6): Flavonols (quercetin, morin, kaempferol, myricetin, rutin, isorhamnetin), Flavones (apigenin, luteolin, primuletin), Flavanones (hesperetin, hesperidin, naringenin, naringin, eriodictyol), Flavanols, also called catechins ((+)-catechin, (+)-gallocatechin, (-)-epicatechin, (-)-epigallocatechin, (-)-epicatechin 3-gallate, (-)-epigallocatechin 3-gallate, theaflavin, theaflavin 3-gallate, theaflavin 3'-gallate, theaflavin 3,3'-digallate, thearubigins), Anthocyanidins (cyanidin, delphinidin, malvidin, pelargonidin, peonidin, petunidin) and Isoflavonoids (genistein and daidzein). Most of these (flavanones, flavones, flavonols, and anthocyanins) bear ring B in position 2 of the heterocyclic ring. In isoflavonoids, ring B occupies position 3.

Although there is strong evidence to suggest beneficial effects of flavonoids in human health, the extent and mechanism by which flavonoids reach the systemic circulation from dietary sources are controversial. Plant flavonoids are predominantly found as β-glycosides with flavonols existing as 3, 7, and 4' *O*-glycosides, whereas other flavonoids, such as flavones, flavonones, and isoflavones, are mainly glycosylated at position 7 (Price et al., 1997; Fossen et al., 1998). Dietary flavonoids are deglycosylated by cytosolic β-glucosidase (CBG) and lactase phlorizin hydrolase (LPH) in the small intestine (Day et al., 1998; Day et al., 2000), followed by conjugation primarily with glucuronic acid in the small intestine epithelial cells (Gee et al., 2000; Crespy et al., 1999; Spencere et al., 1999). Ingested flavonoids undergo extensive Phase I and Phase II metabolism and are present in the circulation as a complex mixture of free aglycone with glucuronidated, methylated, and sulphated forms. However, cleavage by glucuronidases at several sites in the body can restore the aglycone form (Figure 3) (Murota and Terao, 2003) of which shows enhanced ability to partition across membranes and access intracellular sites due to its greater lipophilicity (Spencer et al., 2001).

Several studies have shown that flavonoids can modulate the activities of both P-gp and MRP1 (Zhang and Morris, 2003a; Bobrowska-Hagerstrand et al., 2003) affecting drug accumulation, cell viability following cytotoxic drug exposure, and the ATPase activity of P-gp (Bobrowska-Hagerstrand et al., 2003). Some flavonoids have been reported to interact with the intrinsic ATPase of P-gp, both inhibition and stimulation of P-gp ATPase

activity have been observed for silymarin, morin, and biochanin A (Zhang and Morris, 2003b). Since P-gp located in the apical membrane (Anderle et al., 1998) and some mRNAs of organic cation transporters (OCT) has also been detected (Martel et al., 2001), the monolayer formed by a human colon carcinoma cell line, Caco-2 cell, is used for the study of membrane permeability, specifically for the transport characterization of the intestinal epithelium. Some flavonoids reduced the secretory flux of talinolol across Caco-2 cells, such as hesperetin, quercetin, kaempferol, spiraeoside, isoquercitrin and naringin, but none of the selected flavonoids was able to replace [^{3}H]talinolol from its binding to P-gp, which might be due to an interaction with P-gp without competition of talinolol binding site of P-gp (Ofer et al., 2005). Several flavonoids, specifically methoxylated flavonoids, are confirmed to be the good inhibitors of MRP1 and 2 (van Zanden et al., 2004).

Flavonoids, flavanols, also called catechins, are the major flavonoid found in green tea. Several studies illustrated that tea consumption might provide protection against stroke, osteoporosis, liver disease, and bacterial and viral infections (Mukhtar and Ahmad, 2000). Six catechins present in green tea, the most abundant being (−)-epigallocatechin gallate (EGCG) followed by (−)-epicatechin gallate (ECG), (−)-epigallocatechin (EGC), (−)-epicatechin (EC), (−)-catechin gallate (GC) and (+)-catechin (C) (Chu and Juneja, 1997). The chemical structures of catechins are shown in Figure 14. EGCG has a wide range of biological and pharmacological activities, including antioxidant (Higdon and Frei, 2003), antimutagenic, and anticarcinogenic activities (Kuroda and Hara, 1999). A prospective cohort study of a Japanese population revealed that the daily intake of EGCG in green tea in these subjects was calculated to be 540–720 mg (Muto et al., 2001), which is about 9-12 mg/kg body weight.

EGCG is largely conjugated in the plasma of mice and rats, whereas EGCG exists mostly in free form in human plasma (Chen et al., 1997; Lee et al., 2002). When EGCG at a dose of 10 mg/kg was administered intravenously in rats, the $t_{1/2}$ of 135 min, clearance of 72.5 ml $\cdot kg^{-1} \cdot min^{-1}$ and V_d of 22.5 dl/kg were observed, and EGCG is mainly excreted through bile (Chen et al., 1997). A single oral EGCG at a dose of 3 mg/kg in humans showed T_{max} of 1.3–1.6 h and $t_{1/2}$ of 2.0 h in the plasma (Lee et al., 2002), and the bioavailability of EGCG is low. Chen et al. (1997) reported that the bioavailability of

EGCG in rats after i.g. administration at a dose of 75 mg/kg was 1.6%. Cai et al. (2002) reported that the bioavailability of intraportal administered EGCG was 87%. These results suggests that the limited bioavailability of EGCG is due largely to the factors within the gastrointestinal tract such as limited membrane permeability, transporter mediated intestinal secretion, or gut wall metabolism.

EGCG and its metabolites showed the property to inhibit or substrate for the catalytic enzyme and the ABC transporters. EGCG and ECG inhibited CYP3A4 with the IC_{50} values of 10 and 30 μM, respectively (Muto et al., 2001). In addition, EGCG is a substrate for UDP-glucuronosyltransferase, sulfotransferase, and catechol-*O*-methyltransferase, and there are significant species differences in the amount of EGCG conjugate found in the plasma (Lu et al., 2003a; Lu et al., 2003b). The phase II metabolism and the efflux of EGCG and its metabolites affect the bioavailability of EGCG. According to the report of Hong et al. (2003), the presence of the MRP inhibitors indomethacin increased EGCG, 4″-*O*-methyl EGCG, and 4′,4″-di-*O*-methyl EGCG levels by 13–, 11–, and 3–fold in MDCKII/MRP1 cells, respecitively, and accumulation of EGCG and its methyl metabolites was also increased nearly 10-fold in the presence of MRP inhibitor MK-571 in MDCKII/MRP2 cells. However, they were not affected by GF120918, a third generation P-gp inhibitor, in P-gp overexpressing MDCKII cells, indicating that EGCG and its methyl metabolites are substrates for MRP1 and MRP2, but not for P-gp. Based on the location of MRP2 (apical) and MRP1 (basolateral) in the intestine, kidney and liver, they would act adversely to the bioavailability of their substrates. It was reported that the transcript level of MRP2 was over 10-fold higher than that of MRP1 in the human jejunum (Taipalensuu et al., 2001), MRP2 might also paticipate in lowering the bioavailability of EGCG in the intestine. Although EGCG is not the substrate of P-gp, the inhibitory effect of EGCG on P-gp was observed in human Caco-2 cells. 100 μM of EGCG and the 10 μM PSC 833 (P-gp inhibitor) increased the apical-to-basal flux of [^{3}H] vinblastine across the Caco-2 cell monolayer by 2.6–fold and increased the accumulation of [^{3}H]vinblastine within the cells by 2.2– and 3.4–fold (Jodoin et al., 2002), respectively. EGCG also increased the intracellular accumulation of doxorubicin in human oral epidermoid carcinoma KB-A_1 cells overexpressing P-gp, the expression of *MDR1* mRNA was not changed obviously by increasing EGCG concentrations (Qian et al., 2005). This result indicates that EGCG

increases intracellular drug level by modulating P-gp function, not by down-regulating *MDR1* gene transcription and P-gp expression.

The flavonoid, EGCG, was abundant in our dietary supplements. There are many opportunities that these flavonoids would be administered concomitantly with the agents that are substrates for CYP3A and P-gp in the clinical practice. Since they possess the ability to inhibit CYP3A and P-gp, they might affect the pharmacokinetics of many substrate agents. In this study, the pharmacokinetic behavior of verapamil and norverapamil after intragastric and intravenous administration of verapamil to rats was investigated the effect of EGCG on the oral bioavailability of verapamil and norverapamil in rats.

2. Materials and methods

2.1. Materials

Verapamil, norverapamil, EGCG, and propranolol [an inernal standard for the high-performance liquid chromatographic (HPLC) analysis for verapamil and norverapamil] were purchased from Sigma–Aldrich Corporation (St. Louis, MO, USA). Acetonitrile, triethylamine, and diethylether were products from Merck Corporation (Darmstadt, Germany). Phosphoric acid was obtained from Junsei Corporation (Tokyo, Japan). Other chemicals were of reagent grade.

2.2. HPLC analysis

2.2.1. Instrumentation

A high-performance liquid chromatograph (HPLC) equipped with two solvent delivery pumps (Model LC-10AD; Shimadzu Co., Kyoto, Japan), a fluorescence detector (Model RF-10A), a system controller (Model SCL-10A), degasser (Model DGU-12A) and an autoinjector (SIL-10AD).

2.2.2. Chromatographic conditions

The fluorescence detector was set at an excitation wavelength of 280 nm and an emission wavelength of 310 nm. The stationary phase was a Kromasil KR 100-5C_8 column (5 μm; 4.6 mm, i.d.×250 mm, EKA Chemicals, Sweden) and the mobile phase was acetonitrile:0.05 M KH_2PO_4 with 0.05% triethylamine (30:70, v/v; PH 4.0), which was run at a flow rate of 1.5 ml/min. The coefficient of variation for inter- and intra-day was < 12.5%.

2.2.3. Preparation of stock solutions

Stock solutions of verapamil, norverapamil, and propranolol (an internal standard) were prepared by dissolving 10 mg of each drug in 10 ml of methanol. All solutions were stored at –40°C (MDF-292, Sumwon Company, Seoul, South Korea).

2.2.4. Preparation of analytical standard solutions

Each standard solution, verapamil and norverpamil was prepared by diluting the each stock solution with methanol immediately prior to use. All preparations were made in 1.5-ml polyethylene mocrotubes (Axygen Scientific Company, Calif., USA). The standard solutions of verapamil and norverapamil were all 8, 20, 40, 80, 200, 400 and 800 ng/ml. The concentration of propranolol was 2 ng/ml.

2.2.5. Sample preparation

The plasma concentrations of verapamil and norverapamil were determined by a slight

modified of an HPLC method reported by Choi et al. (2004). Briefly, a 40-µl aliquot of propranolol HCl (400 ng/ml; an internal standard), a 20-µl aliquiot of 2 N sodium hydroxide solution, and 1.2 ml of diethylether were added to a 0.2-ml aliquot of the plasma sample in a 2.0-ml polypropylene microtube (Axygen Scientific Company, Calif., USA). The mixture was mixed vigorously with a vortex-mixer (Scientific Industries Company, NY, USA) for 2 min and centrifuged (13,000 rpm, 10 min) in a micro centrifuge (Hitachi Company, Tokyo, Japan). A 1.0 ml of the organic layer was transferred into a clean micro tube and evaporated at 35^{o}C under a dry thermo bath (Rikakikai Company, Tokyo, Japan). The residue was dissolved in 200 µl of the mobile phase and centrifuged (13,000 rpm, 5 min). A 50-µl aliquot of the supernatant was directly injected onto the HPLC column.

2.2.6. Validation procedures

2.2.6.1. Linearity

Standard calibration curves were constructed by adding a 50-µl aliquot of verapamil and norverapamil standard solutions at the concentrations of 8, 20, 40, 80, 200, 400 and 800 ng/ml, and a 50-µl aliquot of propranolol at a concentration of 2 ng/ml into a 0.2-ml aliquot each rat blank plasma. Thus, the plasma calibrations were 2, 5, 10, 20, 50, 100 and 200 ng/ml for verapamil plus norverapamil. Then, the extraction procedure was followed as described above. Calibration curves of verapamil and norverapamil were constructed using the ratio of the peak area of verapamil or norverapamil with that of propranolol. The linearity was determined by construction of a regression line using the method of least sum of squares.

2.2.6.2. Recovery

To determine the extraction efficiency, a 50-µl aliquot of the standard solutions of verapamil and norverapamil at the concentrations of 5, 20 and 100 ng/ml were added separately to a 0.2-ml aliquot of blank plasma samples to yield concentrations of 5, 20 and 100 ng/ml of verapamil and norverapamil in plasma, respectively. Each of these spiked blank plasma samples were treated as those in the sample preparation. The absolute

recovery was calculated by comparing the peak areas in 50% of methanol in deionized water (n = 5).

2.2.6.3. Intra- and inter-day variability and determination of LOD and LLOQ

Intra-day variability was obtained from five different rat's plasma samples using the same calibration curve in a day. Inter-day variability was obtained on five different days. The mean relative standard deviation (RSD) of the mean predicted concentration for the independently assayed standards provided the measure of precision. Accuracy was calculated by the percentage deviation of the mean predicted concentration of verapamil and norverapamil from the expected target value.

The limit of detection (LOD) was determined by greater than 3.0 for signal to noise (S/N) ratios. The lower limit of quantification (LLOQ) was determined by spiking a 0.2-ml aliquot of blank rat's plasma with verpamil and norverapamil at the concentration of the lowest calibrator with a precision of 20% and accuracy of ± 20%. The LOD and LLOQ were measured on five different days.

The predetermined criteria for acceptance of both intra- and inter-day results were that the standard concentrations of verapamil and norverapamil had to be accurate within ± 15% of their nominal values as determined by the best-fit regression line except for the LLOQ, where ± 20% was acceptable. The correlation coefficient (r^2) also had to be 0.95 or greater.

2.3. Animal experiments

The protocol of this animal study was approved by the Animal Care Committee of Chosun University, Gwangju, South Korea. Male Sprague–Dawley rats, 7–8 weeks old and weighing 270–300 g, were purchased from the Dae Han Laboratory Animal Research Company (EumSung, South Korea) and given free access to a commercial rat chow diet (No. 322-7-1; Superfeed Company, Gangwon, South Korea) and tap water. They were maintained in a clean room (College of Pharmacy, Chosun University) at a temperature of 22 ± 2 °C with a 12-h light/dark cycle and relative humidity of 50–60%. The rats were acclimated under these conditions for at least 1 week.

2.4. Drug administration and sampe collection

2.4.1. Intravenous (i.v.) administration of verapamil

Each rat was fasted for at least 24 h prior to beginning the experiment. The left femoral artery (for blood sampling) and the left femoral vein (for drug administration in the intravenous study) were cannulated using a polyethylene tube (SP45; i.d., 0.58 mm, o.d., 0.96 mm; Natsume Seisakusho Company, Tokyo, Japan) while each rat was under light ether anesthesia. Verapamil injectable (diluted in 0.9% NaCl-injectable solution) at a dose of 3.0 mg/kg was injected (total injection volume of 1.5 ml/kg) over 0.5 min via the femoral vein. A blood sample (0.45 ml) was collected via the femoral artery into heparinized tubes at 0 (control), 0.017 (at the end of the infusion), 0.1, 0.25, 0.5, 1, 2, 3, 4, 8, 12 and 24 h after the injection. A blood sample was centrifuged (13,000 rpm, 5 min), and a 200-μl aliquot of plasma samples were stored at –40˚C until using for the HPLC analysis of verapamil and norverapamil. A 0.4-ml aliquot of 0.9% NaCl-injectable solution was injected through the femoral vein.

2.4.2. Intravenous and oral administration of verapamil

Rats were divided into five groups (n = 6, each); oral groups [9 mg/kg of verapamil dissolved in water (3.0 ml/kg)] without (control) or with 3 or 15 mg/kg of EGCG (mixed in distilled water; total oral volume of 3.0 ml/kg), and an intravenous group (3 mg/kg of verapamil; the same solution used 0.9% NaCl injectable solution; total injection volume of 1.5 ml/kg). A feeding tube was used to administer verapamil and EGCG intra-gastrically. EGCG was administered 30 min prior to oral administration of verapamil. A blood sample (0.45 ml aliquot) was collected into heparinized tubes via the femoral artery at 0, 0.1, 0.25, 0.5, 1, 2, 3, 4, 8, 12 and 24 h for the oral study. Whole blood (approximately 1 ml) collected from untreated rats was infused via the femoral artery at 0.25, 1, 3 and 8 h, respectively, to replace blood loss due to blood sampling. The blood samples were centrifuged (13,000 rpm, 5 min), and a 200-μl aliquot of plasma samples was stored at –40 °C until the HPLC analysis.

2.5. Pharmacokinetic analysis

Plasma concentration data were analyzed by non-compartmental methods using WinNonlin software version 4.1 (Pharsight Corporation, Mountain View, CA, USA). The elimination rate constant (K_{el}) was calculated by the log-linear regression of diltiazem concentration data during the elimination phase and the terminal half-life ($t_{1/2}$) was calculated as $0.693/K_{el}$. The peak concentration (C_{max}) of diltiazem in plasma and the time to reach C_{max} (t_{max}) were obtained by visual inspection of the data from the concentration–time curve. The area under the plasma concentration–time curve (AUC) from time zero to the time of last measured concentration (C_{last}) was calculated by the linear trapezoidal rule. The AUC zero to infinity ($AUC_{0-\infty}$) was obtained by adding AUC_{0-t} and the extrapolated area determined by C_{last}/K_{el}. The total body clearances of oral (CL/F) diltiazem were calculated from the quotient of the dose (D) and the $AUC_{0-\infty}$ of the intravenous and oral routes. The extent of absolute oral bioavailability (F) was calculated by $AUC_{0-\infty}$ after oral administration by $AUC_{0-\infty}$ afrer intravenous administration. The relative bioavailability (RB) of verapamil was calculated by $AUC_{\text{verapamil with}}/AUC_{\text{verapamil without}}$. The metabolite–parent ratio (MR) was calculated by $AUC_{\text{norverapamil}}/AUC_{\text{verapamil}}$.

2.6. Statistical analysis

The pharmacokinetic parameters were compared using a one-way ANOVA, followed by a posteriori testing with the Dunnett correction. Differences were considered significant at a level of $p < 0.05$. All data are expressed in terms of mean ± S.D.

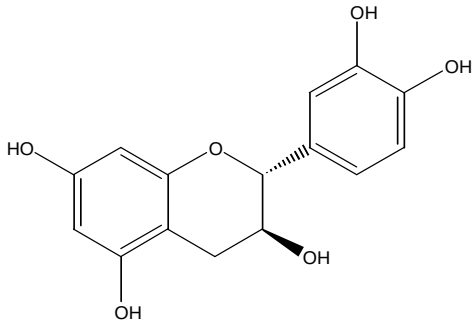

(+)-Catechin (C)

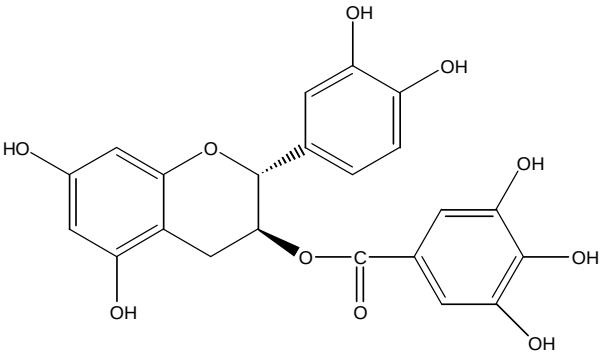

(-)-catechin gallate (CG)

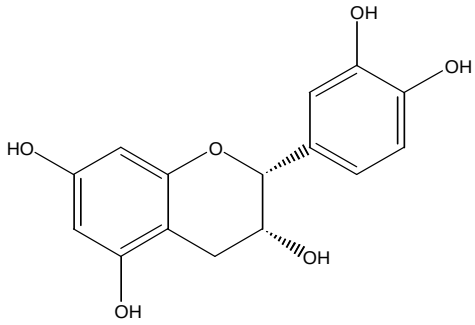

(-)-epicatechin (EC)

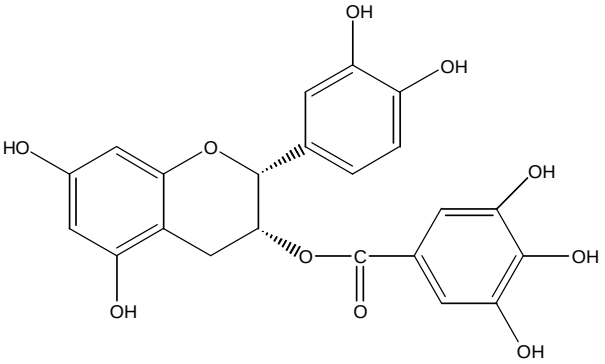

(-)-epicatechin gallate (ECG)

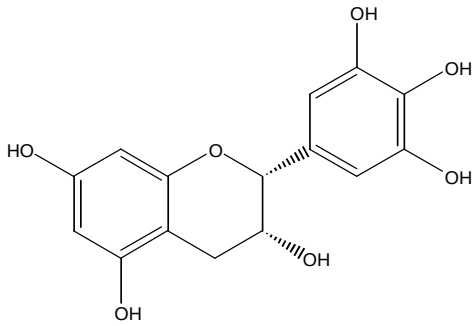

(-)-epigallocatechin (EGC)

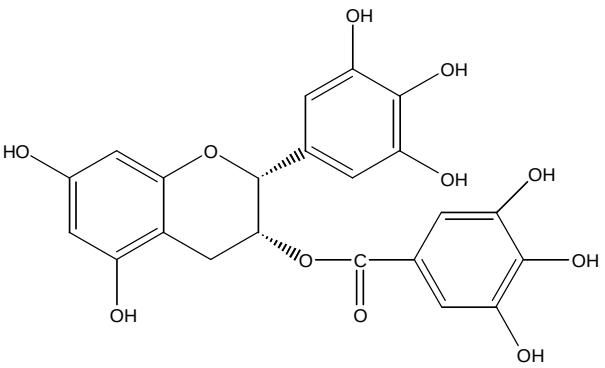

(-)-epigallocatechin gallate (EGCG)

Figure 14. Chemical structures of catechins.

3. Results and Discusssion

Figure 9 depicts the chromatograms of blank rat plasma sample (A), plasma sample collected (0.5 hour) after oral administration of verapamil (B) to rats. The retention times of propranolol (an internal standard, IS), verapamil, and norverapamil were 4.7, 16, and 13.9 min, respectively. The overall run time lasted 18 min.

Calibration curves for verapamil (Figure 10) and norverapamil (Figure 11) constructed by plotting the ratio of the peak area of verapamil or norverpamil to that of propranolol as a function of the plasma verapamil or norverapamil concentrations (2, 5, 10, 20, 50, 100 and 200 ng/ml). There is a good linearity over the range of 2–200 ng/ml with a mean correlation coefficient of 0.997 (verapamil) and 0.998 (norverapamil). The typical equation describing the calibration curve in rat's plasma was $y = 0.0232\ x + 0.1297$ (for verpamil) and $y = 0.0195\ x - 0.0663$ (for norverpamil), where y is the peak area ratio of verapamil or norverpamil to propranolol and x is the concentration of verapamil or norverpamil, respectively.

The recovery of verpamil or norverapamil after liquid-liquid extraction procedure was evaluated at three concentrations (5, 20 and 100 ng/ml, respectively). The recovery of the verapamil and norverapamil was above 84.3–88.0% and 82.6–83.9%, respectively, when spiked concentration in rat plasma was 2.0 ng/ml (Table 1).

The LOD for verapamil or norverapamil in rat plasma defined as a s/n ratio of greater than 3 was 2 ng/ml. The LLOQ for verapamil (Table 2) was 2 ng/ml with an acceptable precision and accuracy (RSD: 12.6%, deviation: −8.5%, n = 5). The LLOQ for norverapamil (Table 3) was 2 ng/ml with an acceptable precision and accuracy (RSD: 13.1%, deviation: −10%, n = 5).

Figure 15 depicts the mean plasma concentration–time profiles of verapamil after oral administration (9 mg/kg) of verapamil with or without EGCG (3 or 15 mg/kg). Table 10 lists the pharmacokinetic parameters of verapamil after oral administration. EGCG (3 or 15 mg/kg) significantly ($p < 0.01$) increased the AUC and the C_{max} of verapamil by 85.2–127% and 102–136%, respectively, and EGCG increased the $t_{1/2}$ of norverapamil but not significantly. EGCG significantly ($p < 0.01$) decreased the CL/F of verapamil by 46.0–55.9%. Consequently, the F of verapamil in control group was 5.15%, which was

increased significantly by 9.52–11.7%, and the RB of verapamil increased by 1.85- to 2.27-fold. Verapamil is known to be a substrate P-gp and CYP3A4 (Doppenschmitt et al., 1999; Saitoh and Aungst, 1995). EGCG was reported to be a dual inhibitor of CYP3A4 (Muto et al., 2001) and P-gp in human Caco-2 cells (Jodoin et al., 2002). Kitagawa et al. (2004) also reported that EGCG inhibited the efflux of verapamil in KB-C2 cell. These results were consistent with the results reported by Choi et al., in that flavonoid (quercetin, naringin, morin), an inhibitor of CYP3A and P-gp, significantly enhanced the oral bioavailability of verapamil and diltiazem in rabbits (Choi and Han, 2004; Kim and Choi, 2005; Choi and Li, 2005). Hong et al. (2003) reported that EGCG and its methyl metabolites are substrates for MRP1 and MRP2, these transporters might affect the first-pass extraction of verapamil. EGCG showed no significant changes the K_{el} and T_{max} of verapamil.

Figure 16 depicts the mean plasma concentration–time profiles of norverapamil after oral administration (9 mg/kg) of verapamil with or without EGCG (3 or 15 mg/kg). As lists in Table 11, EGCG significantly altered the pharmacokinetic parameters of norverapamil in this study. Compared with the control group, the presence of 3 or 15 mg/kg of EGCG significantly ($p < 0.01$) increased the AUC (72.9–93.9%) and C_{max} (65.3–72.9%), respectively. EGCG was increased the $t_{1/2}$ of norverapamil but not significantly, and the R.B. of norverapamil increased by 1.73- to 1.94-fold. Norverapamil and D-617 are substrate and inhibitor of P-gp (Pauli-Magnus et al., 2000; Woodland et al., 2003).These results suggest the metabolism and excretion of norverapamil in the liver and kidney must be inhibited by 3 or 15 mg/kg of EGCG. Given that EGCG can either inhibit or stimulate human CYPs depending upon their structures, concentrations, and experimental conditions, which might be due to the low plasma concentration of EGCG to inhibit CYP3A and P-gp in the liver and intestine. EGCG showed no significant changes in the MR, K_{el} and T_{max} of norverapamil.

Orally administered drugs must pass through the small intestinal membrane to access the systemic circulation (Figure 3). Like other lipophilic drugs, most of verapamil is absorbed via the apical enterocytes of the villi of small intestine where full of CYP3A and P-gp rather than via the deep crypts with low level of CYP3A and P-gp or the splanchnic capillaries by paracellular transport, which attribute to the considerable exposure of

verapamil in CYP3A and P-gp of the enterocyte (Figure 3). Second, although the protein binding is not correlated with the exposure in the enterocytes, it is of magnitude for the exposure in the hepatocytes because only free form can pass through the sinusoidal membrane of hepatocytes. The high level protein binding of verapamil (90%) should be one of the contributors to its low hepatic first-pass effect (Schomerus et al., 1976). Last, the blood flow rate in the liver is 55.2 ml/min/kg in rats, and in the value the gut is 30 ml/min/kg (Davies and Morris, 1993). Thus, the blood flow rate in the small intestine is considerably lower than that in the liver. The slower of blood flow rate would increase residence time of verapami in the intestine during first-pass compared to hepatocyte, which can be another contributor to the high intestinal first-pass extraction of verapamil than the liver. Choi and Han (2004) reported that quercetin, a dual inhibitor of CYP3A and P-gp, significantly enhanced the F of verapamil in rats. The factors within the gastrointestinal tract such as transporter mediated intestinal secretion, or gut wall metabolism may contribute considerably to the variable oral F of verapamil.

The involvement of P-gp in risperidone disposition has recently been documented (Boulton et al., 2002, Wang et al., 2004 and Nakagami et al., 2005). In the intestine, P-gp is expressed on the brush-border membrane of enterocytes and pumps compounds out of cells from the cytosol to the intestinal lumen. P-gp has been labelled a transport barrier to the oral absorption of drugs (Leu and Huang, 1995, Fricker et al., 1996, Lown et al., 1997, Kim et al., 1998 and Salphati and Benet, 1998). Moreover, P-gp could act along with CYP3A4 to increase drug presystemic metabolism (Gan et al., 1996, Watkins, 1997, Wacher et al., 1998 and Ito et al., 1999). The above mentioned two mechanisms have been proposed to explain how P-gp may enhance the extent of intestinal absorption. According to a first mechanism, P-gp activity induces repeated cycles of secretion of drug into the intestinal lumen, resulting in repeated cycles of absorption. The residence time of a drug in the intestine and its exposure to intestinal CYP3A4 are lengthened prior to systemic absorption (Gan et al., 1996). A second mechanism has been proposed suggesting that P-gp may facilitate the removal of intracellular primary metabolites, thus minimising the potential to produce CYP3A4 inhibition (Lown et al., 1997).

The increased bioavailability of verapamil by EGCG suggests that CYP3A and P-gp could be inhibited by EGCG, which resulted in reducing first-pass metabolism of

verapamil. In the above mentioned results were consistent with the results reported by Choi et al. (2004), in that flavonoid (quercetin) significantly enhanced the oral bioavailability of verapamil in rabbits (Choi and Han, 2004). And similar to our previous study (Choi and Han 2005), morin inhibited P-gp and CYP3A, enhanced absorption of verapamil in rats.

Table 8. Mean (± S.D.) plasma concentrations of verapamil after its intravenous or oral

administration of verapamil at a dose of 9 mg/kg with or without EGCG at a dose of 3 or 15 mg/kg to rats (n = 6, each).

Time (h)	Control (oral)	Verapamil + EGCG		Verapamil (i.v.)
		3 mg/kg	15 mg/kg	
0	0	0	0	4836 ± 62.1
0.1	35 ± 8.4	42.0 ± 57.2	49.0 ± 80.8	1432 ± 62.1
0.25	58 ± 14	89.0 ± 73.2	103 ± 132.6	1025 ± 87.5
0.5	56 ± 13.8	117 ± 115.5	137 ± 118.4	676 ± 90.6
1	36 ± 8.6	81.0 ± 149.6	96.0 ± 101.5	367 ± 78.4
2	24 ± 6.0	44.0 ± 157.6	53.0 ± 74.5	158 ± 74.4
3	17 ± 4.1	26.0 ± 91.9	33.0 ± 74.4	88 ± 58.3
4	11 ± 2.4	18.5 ± 27.8	23.3 ± 24.7	45 ± 15.3
8	7.2 ± 1.7	12.7 ± 11.7	15.5 ± 16.0	16.1 ± 11.9
12	5.0 ± 1.2	8.6 ± 7.49	10.7 ± 11.4	7.2 ± 8.06
24	2.6 ± 0.63	5.1 ± 5.89	6.4 ± 8.04	2.5 ± 6.27

Table 9. Mean (± S.D.) plasma concentrations of norverapamil after oral administration of

verapamil at a dose of 9 mg/kg with or without EGCG at a dose of 3 or 15 mg/kg to rats (n = 6, each).

Time (h)	Control	Verapamil + EGCG	
		3 mg/kg	15 mg/kg
0	0	0	0
0.1	12.3 ± 2.92	16.7 ± 3.91	17.8 ± 4.15
0.25	29.4 ± 7.21	39.2 ± 9.22	42.2 ± 9.77
0.5	37.1 ± 9.05	62 ± 14.2	64.9 ± 14.9
1	38.0 ± 9.41	62.8 ± 14.3	65.7 ± 15.2
2	23.7 ± 5.81	38.7 ± 9.02	41.4 ± 9.57
3	16.5 ± 4.02	27.1 ± 6.35	29.2 ± 6.72
4	11.9 ± 2.76	17.7 ± 4.28	19.6 ± 4.53
8	7.8 ± 1.84	13.0 ± 3.15	14.5 ± 3.34
12	5.4 ± 1.15	8.8 ± 2.09	9.7 ± 2.23
24	2.8 ± 0.69	5.3 ± 1.33	6.2 ± 1.43

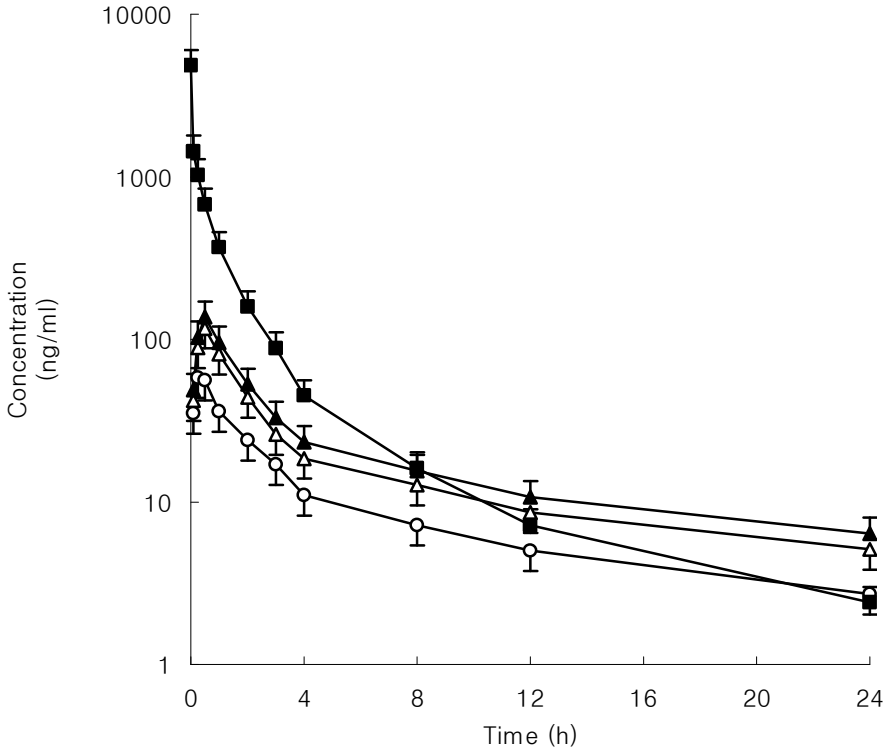

Figure 15. Mean plasma concentration–time profiles of verapamil following intravenous (3 mg/kg) or oral (9 mg/kg) administration of verapamil to rats with or without EGCG (Mean ± S.D. n = 6). (○) Control (verapamil 9 mg/kg, oral); (△) the presence of 3 mg/kg of EGCG; (▲) the presence of 15 mg/kg of EGCG; (■) i.v. injection of verapamil 3 mg/kg. Bars represent the standard deviation.

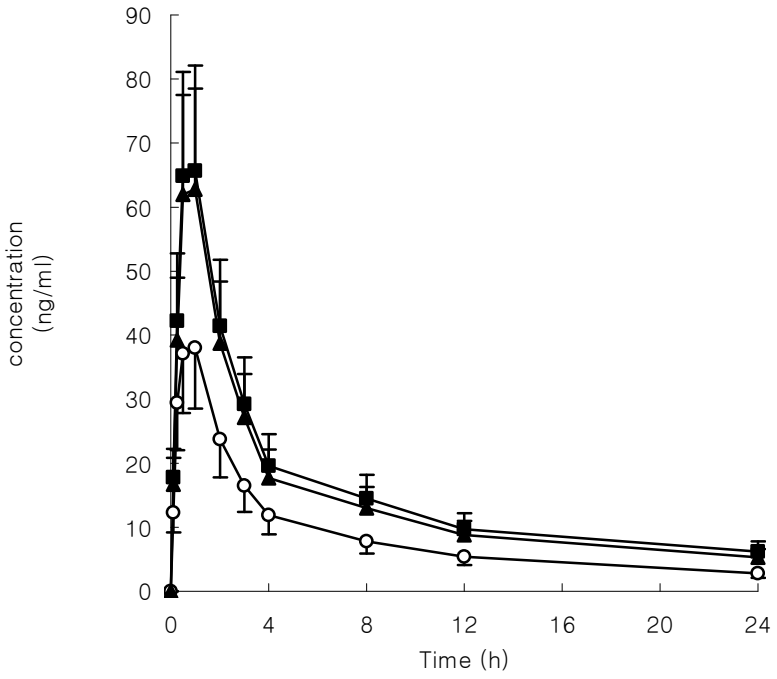

Figure 16. Mean plasma concentration–time profiles of norverapamil after oral administration of verapamil (9 mg/kg) to rats with or without EGCG (Mean ± S.D., n = 6). (○) Control (verapamil 9 mg/kg, oral), (△) the presence of 3 mg/kg of EGCG, (▲) the presence of 15 mg/kg of EGCG. Bars represent the standard deviation.

Table 10. Mean (± S.D.) pharmacokinetic parameters of verapamil after intravenous or oral administration of verapamil at a dose of 9 mg/kg with or without EGCG at a dose of 3 or 15 mg/kg to rats (n = 6, each).

Parameter	Control (oral)	Verapamil + EGCG		Verapamil (i.v.)
		3 mg/kg	15 mg/kg	
AUC (ng·h/ml)	257 ± 58	476 ± 102**	583 ± 132**	1667 ± 403
C_{max} (ng/ml)	58 ± 14	117 ± 28.6**	137 ± 32.5**	-
T_{max} (h)	0.25	0.5	0.5	-
CL/F	583 ± 150	315 ± 74.6**	257 ± 57.2**	-
K_{el} (h)	0.068 ± 0.016	0.062 ± 0.015	0.062 ± 0.015	0.139 ± 0.031
$t_{1/2}$ (h)	10.0 ± 2.4	11.1 ± 2.7	11.2 ± 2.8	5.1 ± 1.12
F (%)	5.15	9.52	11.7	-
RB (%)	100	185	227	-

**p < 0.01; compared to control.

AUC: area under the plasma concentration–time curve from 0 to 24 h

C_{max}: peak concentration

CL/F: total plasma clearence

K_{el}: elimination rate constant

$t_{1/2}$: terminal half-life

T_{max}: time to reach peak concentration

F: absolute oral bioavailability

RB: relative bioavailability, ratio

Table 11. Mean (± S.D.) pharmacokinetic parameters of norverapamil after oral administration of verapamil at a dose of 9 mg/kg with or without EGCG at a dose of 3 or 15 mg/kg to rats (n = 6, each).

Parameter	Control (oral)	Verapamil + EGCG	
		3 mg/kg	15 mg/kg
AUC (ng·h/ml)	251 ± 64	434 ± 109**	486 ± 120**
C_{max} (ng/ml)	38.0 ± 9.01	62.8 ± 13.6**	65.7 ± 14.8**
T_{max} (h)	1.0	1.0	1.0
$t_{1/2}$ (h)	9.91 ± 2.5	11.7 ± 2.7	12.3 ± 2.7
K_{el} (h)	0.070 ± 0.018	0.059 ± 0.016	0.056 ± 0.016
MR	0.98 ± 0.25	0.91 ± 0.24	0.83 ± 0.22
RB (%)	100	173	194

**p < 0.01; compared to control.

AUC: area under the plasma concentration–time curve from 0 to 24 h

C_{max}: peak concentration

K_{el}: elimination rate constant

$t_{1/2}$: terminal half-life

T_{max}: time to reach peak concentration

RB: relative bioavailability

MR: Metbolite Parent ratio

4. Conclusion

A flavonoid, epigallocatechin gallate, enhanced the oral bioavailability of verapamil.

Because epigallocatechin gallate have many health-promoting benefits and have no consistent side effects, it might be available as the MDR modulators in the clinical therapy to improve the F of verapamil in humans.

References

Adachi Y, Suzuki H, Sugiyama Y. Comparative studies on *in vitro* methods for evaluating *in vivo* function of MDR1 P-glycoprotein. Pharm. Res. 2001; 18: 1660–1668.

Ameer B, Weintraus RA, Johnson JV, Yost RA, Rouseff RL. Flavanone absorption after naringin, hesperidin, and citrus administration. Clin. Pharmacol. Ther. 1996; 60: 34–40.

Anderle P, Niederer E, Rubas W, Hilgendorf C, Spahn-Langguth H, Wunderli-Allenspach H, Merkle HP, Langguth P. P-glycoprotein (P-gp) mediated efflux in Caco-2 cell monolayers: the influence of culturing conditions and drug exposure on P-gp expression levels.J. Pharm. Sci. 1998; 87: 757–762.

Barthe GA, Jourdan PS, Mclntosh Ca, Mansell RL. Radioimmunoassay for the quantitative determination of hesperidin and analysis of its distribution in citrus sinensis. Phytochemistry. 1988; 27: 249–254

Bobrowska-Hagerstrand M, Wrobel A, Mrowczynska L, Soderstrom T, Shirataki Y, Motohashi N, Molnar J, Michalak K, Hagerstrand H. Flavonoids as inhibitors of MRP1-like efflux activity in human erythrocytes. A structure–activity relationship study. Oncol. Res. 2003; 13: 463–469.

Bok SH, Lee SH, Park YB, Bae KH, Son KH, Jeong TS, Choi MS. Plasma and hepatic cholesterol and hepatic activities of 3-hydroxy-3-methyl-glutaryl-CoA reductase and acyl CoA: cholesterol transferase are lower in rats fed citrus peel extract or a mixture of citrus bioflavonoids. J. Nutr. 1999; 129: 1182–1185.

Borradaile NM, Carroll KK, Kurowska EM. Regulation of HepG2 cell apolipoprotein B metabolism by the citrus flavanones hesperetin and naringenin. Lipids. 1999; 34: 591–598.

Boulton DW, DeVane CL, Liston HL, Markowitz JS. *In vitro* P-glycoprotein affinity for atypical and conventional antipsychotics. Life Sci. 2002; 71: 163–169.

Bruggemann EP, Currier SJ, Gottesman MM, Pastan I. Characterization of the azidopine and vinblastine binding site of P-glycoprotein. J. Biol. Chem. 1992; 267: 21020–21026

Bruggemann EP, Germann UA, Gottesman MM, Pastan I. Two different regions of P-glycoprotein [corrected] are photoaffinity-labeled by azidopine. J. Biol. Chem. 1989; 264: 15483–15488

Buchler M, Konig J, Brom M, Kartenbeck J, Spring H, Horie T, Keppler D. cDNA cloning of the hepatocyte canalicular isoform of the multidrug resistance protein,

cMrp, reveals a novel conjugate export pump deficient in hyperbilirubinemic mutant rats. J. Biol. Chem. 1996; 271: 15091–15098.

Cai Y, Anavy ND, Chow HH. Contribution of presystemic hepatic extraction to the low oral bioavailability of green tea catechins in rats. Drug Metab. Dispos. 2002; 30: 1246–1249.

Cherrington NJ, Hartley DP, Li N, Johnson DR, Klaassen CD. Organ distribution of multidrug resistance proteins 1, 2, and 3 (Mrp1, 2, and 3) mRNA and hepatic induction of Mrp3 by constitutive androstane receptor activators in rats. J .Pharmacol. Exp. Ther. 2002; 300: 97–104.

Chen L, Lee MJ, Li H, Yang CS. Absorption, distribution, elimination of tea polyphenols in rats. Drug Metab. Dispos. 1997; 25: 1045–1050.

Chu DC, Juneja LR. In: Yamanoto T, Juneja LR, Chu DC, Kim M. (Eds.), Chemistry and Applications of Green Tea, CRC Press, New York. 1977, pp.13–22.

Crespy V, Morand C, Manach C, Besson C, Demigne C, Remesy C. Part of quercetin absorbed in the small intestine is conjugated and further secreted in the intestinal lumen. Am. J. Physiol. 1999; 277: G120–G126.

Day AJ, Dupont MS, Ridley S, Rhodes M, Rhodes MJC, Morgan MRA, Williamson G. Deglycosylation of flavonoid and isoflavonoid glycosides by human small intestine and liver ß-glucosidase activity. FEBS Lett. 1998; 436: 71–75.

Day AJ, Canada FJ, Diaz JC, Kroon PA, McLauchlan R, Faulds CB, Plumb G, Morgan MRA, Williamson G. Dietary flavonoid and isoflavone glycosides are hydrolysed by the lactase site of lactase phlorizin hydrolase. FEBS Lett. 2000; 468: 166–170.

Devault A, Gros P. Two members of the mouse mdr gene family confer multidrug resistance with overlapping but distinct drug specificities. Mol. Cel. Biol. 1990; 10: 1652–1663

Devine SE, Hussain A, Davide JP, Melera PW. Full length and alternatively spliced pgp1 transcripts in multidrug-resistant Chinese hamster lung cells. J. Biol. Chem. 1991; 266: 4545–4555.

Doppenschmitt S, Spahn-Langguth H, Regardh CG, Langguth P. Role of P-glycoprotein-mediated secretion in absorptive drug permeability: An approach using passive membrane permeability and affinity to P-glycoprotein. J. Pharm. Sci. 1999; 88, 1067–1072.

Eichelbaum M, Mikus G, Vogelgesang B. Pharmacokinetics of (+)-,(−)- and

(±)-verapamil after intravenous administration. Brit. J. Clin. Pharmacol. 1984; 17: 453–458.

Eichelbaum M, Remberg EG, Schomerus M, Dengler HJ. The metabolism of D,L(14C) verapamil in man. Drug Metab. Dispos. 1979; 7: 145–148.

Evans WC. 1996. In *Trease and Evans` Pharmacognosy*. Saunders WB: The Alden Press, Oxford, UK.

Flens MJ, Zaman GJ, van der Valk P, Izquierdo MA, Schroeijers AB, Scheffer GL, van der Groep P, de Haas M, Meijer CJ, Scheper RJ. Tissue distribution of the multidrug resistance protein. Am. J. Pathol. 1996; 148: 1237–1247.

Fojo AT, Ueda K, Slamon DJ, Poplack DG, Gottesman MM, Pastan I. Expression of a multidrug-resistance gene in human tumors and tissues. Proc. Natl. Acad. Sci. USA 1987; 84: 265–269.

Fossen T, Pedersen AT, Anderson OM. Flavonoids from red onion (Allium cepa). Phytochemistry. 1998; 47: 281–285.

Fricker G, Drewe J, Huwyler J, Gutmann H, Beglinger C. Relevance of p-glycoprotein for the enteral absorption of cyclosporin A: *in vitro–in vivo* correlation. Br. J. Pharmacol. 1996; 118: 1841–1847.

Fromm MF, Kauffman HM. Fritz P, Burk O, Kroemer HK, Warzok RW, Eichelbaum M, Siegmund W, Schrenk D. The effect of rifampin treatment on intestinal expression of human MRP transporters. Am. J. Pathol. 2000; 157: 1575–1580.

Gatmaitan ZC, Arias IM. Structure and function of P-glycoprotein in normal liver and small intestine. Adv. Pharmacol. 1993; 24: 77–97.

Garg A, Garg S, Zaneveld LJD, Singla AK. Chemistry and pharmacology of the citrus bioflavonoid hesperidin. Phytother. Res. 2001; 15, 655–669.

Gan LSL, Moseley MA, Khosla B, Augustijns PF, Bradshaw TP, Hendren RW. CYP3A-Like cytochrome P450-mediated metabolism and polarized efflux of cyclosporin A in Caco-2 cells: interaction between the two biochemical barriers to intestinal transport. Drug Metab. Dispos. 1996; 24: 344–349.

Gee JM, DuPont MS, Day AJ, Plumb GW, Williamson G, Johnson IT. Intestinal transport of quercetin glycosides in rats involves both deglycosylation and interaction with the hexose transport pathway. J. Nutr. 2000; 130: 2765–2771.

Gould BA, Mann S, Kieso H, Bala Subramanian V, Raftery EB. The 24-hour ambulatory blood pressure profile with verapamil. Circulation. 1982; 65, 22–27.

Gottesman MM, Pastan I. Biochemistry of multidrug resistance mediated by the multidrug transporter. Annu. Rev. Biochem. 1993; 62: 385–427.

Gros P, Raymond M, Bell J, Housman DE. Cloning and characterization of a second member of the mouse mdr gene family. Mol. Cell. Biol. 1988; 8: 2770–2778

Guengerich FP. Human cytochrome P450 enzymes. In: Ortiz de Montellano P. (Ed.). Cytochrome P450. Plenum. Press, New York. 1995; 473–535.

Gushchin GV, Gushchin MI, Gerber N, Boyd RT. A Novel Cytochrome P450 3A Isoenzyme in Rat Intestinal Microsomes. Biochemical and Biophysical. Research Communications. 1999; 255: 394–398.

Ha PT, Sluyts I, Van Dyck S, Zhang J, Gilissen RA, Hoogmartens J, Van Schepdael A. Chiral capillary electrophoretic analysis of verapamil metabolism by cytochrome P450 3A4. J. Chroma. A. 2006; 1120: 94–101.

Hamann SR, Blouin RA, McAllister RG Jr. Clinical pharmacokinetics of verapamil. Clin. Pharmacokinet. 1984; 9: 26–41.

Hayashi M, Tomita M, Awzu S. Transcellular and paracellular contribution to transport processes in the colorectal route. Adv. Drug Deliv. Rev. 1997; 28: 191–204.

Hertog MGL, Hollman PCH, Katan MB. Content of potentially anticarcinogenic flavonoids of 28 vegetables and 9 fruits commonly consumed in the Netherlands. J. Agric. Food Chem. 1992; 40: 2379–2383.

Hertog MG, Hollman PC, Katan MB, Kromhout D. Intake of potentially anticarcinogenic flavonoids and their determinants in adults in The Netherlands. Nutr. Cancer. 1993a; 20: 21–29.

Hertog MG, Feskens EJ, Hollman PC, Katan MB, Kromhout D. Dietary antioxidant flavonoids and risk of coronary heart disease: the Zutphen Elderly Study. Lancet. 1993b; 342: 1007–1011.

Hertog MG, Kromhout D, Aravanis C, Blackburn H, Buzina R, Fidanza F, Giampaoli S, Jansen A, Menotti A, Nedeljkovic S, et al. Flavonoid intake and long-term risk of coronary heart disease and cancer in the seven countries study. Arch Intern Med 1995; 155: 381–386.

Higdon JV, Frei B. Tea catechins and polyphenols: health effects, metabolism, and antioxidant functions. Crit. Rev. Food Sci. Nutr. 2003; 43: 89–143.

Hodek P, Trefil P, Stiborova M. Flavonoids-potent and versatile biologically active compounds interacting with cytochromes P450. Chem. Biol. Interact. 2002; 139: 1–21.

Hong J, Lambert JD, Lee SH, Sinko PJ, Yang CS. Involvement of multidrug resistance-associated proteins in regulating cellular levels of (-)-epigallocatechin-3-gallate and its methyl metabolites. Biochem. Biophys. Res. Commun. 2003; 310: 222–227.

Hunter J, Hirst BH. Intestinal secretion of drugs. The role of P-glycoprotein and related drug efflux systems in limiting oral drug absorption. Adv. Drug. Del. Rev. 1997; 25: 129–157.

Ito K, Kusuhara H, Sugiyama Y. Effects of intestinal CYP3A4 and P glycoprotein on oral drug absorption theoretical approach. Pharm. Res. 1999; 16: 225–231.

Jodoin J, Demeule M, Beliveau R. Inhibition of the mutldrug resistance P-glycoprotein activity by green tea polyphenols. Biochim. Biophys Acta 2002; 1542: 149–159.

Kaminsky LS, Fasco MJ. Small intestinal cytochromes P450. Crit. Rev. Toxicol. 1991; 21: 407–422.

Kang D, Verotta D, Krecic-Shepard ME, Modi NB, Gupta SK, Schwartz JB. Population analyses of sustained-release verapamil in patients: effects of sex, race, and smoking. Clin. Pharmacol. Ther. 2003; 73: 31–40.

Kelly JG, O'Malley K. Clinical pharmacokinetics of calcium antagonists. An. update. Clin. Pharmacokinet. 1992; 22: 416–433.

Keppler D, Cui Y, Konig J, Leier I, Nies A. Export pumps for anionic conjugates encoded by MRP genes. Adv. Enzyme Regul. 1999; 39: 237–246.

Kim RB, Fromm MF, Wandel C, Leake B, Wood AJJ, Roden DM. The drug transporter P-glycoprotein limits oral absorption and brain entry of HIV-1 protease inhibitors, J. Clin. Invest. 1998; 101: 289–294.

Kirk CR, Gibbs JL, Thomas R, Radley-Smith R, Qureshi SA. Cardiovascular collapse after verapamil in supraventricular tachycardia. Arch. Dis. Child. 1987; 62: 1265–1266.

Korthuis RJ, Gute DC. Adhesion molecule expression in postischemic microvascular dysfunction: activity of a micronized purified flavonoid fraction. J. Vasc. Res. 1999; 36, 15–23.

Kuroda Y, Hara Y. Antimutagenic and anticarcinogenic activity of tea polyphenols. Mutat. Res. 1999; 436: 69–97.

Lee MJ, Maliakal P, Chen L, Meng X, Bondoc FY, Prabhu S, Lambert G, Mohr S, Yang CS. Pharmacokinetics of tea catechins after ingestion of green tea and (-)-epigallocatechin-3-gallate by humans: formation of different metabolites and

individual variability. Cancer Epidemiol. Biomarkers. Prev. 2002; 11: 1025–1032.

Lewis GR, Morley KD, Lewis BM, Bones PJ. The treatment of hypertension with verapamil. NZ. Medical. J. 1978; 87, 351–354.

Leu BL, Huang JD. Inhibition of intestinal P-glycoprotein and effects on etoposide absorption, Cancer Chemother. Pharmacol. 1995; 35: 432–436.

Levy RH, Thummel KE, Trager WF, Hansten PD, Eichelbaum M. Metabolic Drug Interaction. Lippincott William & Wilkins: Philadelphia, PA. 2000; 341.

Lown KS, Mayo RR, Leichtman AB, Hsiao HL, Turgeon DK, Schmiedlin-Ren P. Role of intestinal glycoprotein (mdr-1) in interpatient variation in the oral bioavailability of cyclosporine, Clin. Pharmacol. Ther. 1997; 62: 248–260.

Lu H, Meng X, Yang CS. Enzymology of methylation of tea catechins and inhibition of catechol-*O*-methyltransferase by (−)-epigallocatechin gallate. Drug Metab. Dispos. 2003a; 31: 572–579.

Lu H, Meng X, Li C, Sang S, Patten C, Sheng S, Hong J, Bai N, Winnik B, Ho CT, Yang CS. Glucuronides of tea catechins: enzymology of biosynthesis and biological activities. Drug Metab. Dispos. 2003b; 31: 452–461.

Martel F, Grundemann D, Calhau C, Schomig E. Apical uptake of organic cations by human intestinal Caco-2 cells: putative involvement of ASF transporters. Naunyn. Schmiedebergs Arch. Pharmacol. 2001; 363: 40–49.

Mayer R, Kartenbeck J, Buchler M, Jedlitschky G, Leier I, Keppler D. Expression of the MRP gene-encoded conjugate export pump in liver and its selective absence from the canalicular membrane in transport-deficient mutant hepatocytes. J. Cell Biol. 1995; 131: 137–150.

Middleton EJ. The flavonoids. Trends Pharmacol. Sci. 1984; 8: 335–338.

Mukhtar H, Ahmad N. Tea polyphenols: prevention of cancer and optimizing health. Am. J. Clin. Nutr. 2000; 71: 1698S–1702S.

Murota K, Terao J. Antioxidative flavonoid quercetin: implication of its intestinal absorption and metabolism. Arch. Biochem. Biophys. 2003; 417: 12–17.

Muto S, Fujita K, Yamazaki Y, Kamataki T. Inhibition by green tea catechins of metabolic activation of procarcinogens by human cytochrome P450. Mutat. Res. 2001; 479: 197–206.

Nakagami T, Yasui-Furukori N, Saito M, Tateishi T, Kaneo S. Effect of verapamil on pharmacokinetics and pharmacodynamics of risperidone: *in vivo* evidence of

involvement of P-glycoprotein in risperidone disposition, Clin. Pharmacol. Ther. 2005; 78: 43–51.

Nartowicz E, Burduk P, Ukleja-Adamowicz M, Orzalkiewicz Z, Klobukowski A. Verapamil in the treatment of paroxysmal supraventricular arrhythmia. Kardiol. Pol. 1987; 30: 92–96.

Ofer M, Wolffram S, Koggel A, Spahn-Langguth H, Langguth P. Modulation of drug transport by selected flavonoids: Involvement of P-gp and OCT? Eur. J. Pharm. Sci. 2005; 25: 263–271.

Ozvegy C, Litman T, Szakacs G, Nagy Z, Bates S, Varadi A, Sarkadi B. Functional characterization of the human multidrug transporter, ABCG2, expressed in insect cells. Biochem. Biophys. Res. Commun. 2001; 285: 111–117.

Pauli-Magnus C, von Richter O, Burk O, Ziegler A, Mettang T, Eichelbaum M, Fromm MF. Characterization of the major metabolites of verapamil as substrates and inhibitors of P-glycoprotein. J. Pharmacol. Exp. Ther. 2000; 293: 376–382.

Peng KC, Cluzeaud F, Bens M, van Huyen JP, Wioland MA, Lacave R, Vandewalle A. Tissue and cell distribution of the multidrug resistance-associated protein (MRP) in mouse intestine and kidney. J. Histochem. Cytochem. 1999; 47: 757–768.

Perrot B, Danchin N, Terrier de la Chaise A. Verapamil: a cause of sudden death in a patient with hypertrophic cardiomyopathy. Br. Heart. J. 1984; 51: 352–354.

Preston RK, Avakian S, Beiler JM, Moss JN, Martin GJ. In-vivo and in-vitro inhibition of hyaluronidase by organic phosphates. Exp. Med. Surg. 1953; 11: 1–8.

Price KR, Rhodes MJC. Analysis of the major flavonol glycosides present in four varieties of onion (Allium cepa) and changes in composition resulting from autolysis. J. Sci. Food Agric. 1997; 74: 331–339.

Price KR, Bacon JR, Rhodes MJC. Effect of storage and domestic processing on the content and composition of flavonol glucosides in onions (Allium cepa). J. Agric. Food Chem. 1997; 45: 938–942.

Qian F, Wei D, Zhang Q, Yang S. Modulation of P-glycoprotein function and reversal of multidrug resistance by (-)-epigallocatechin gallate in human cancer cells. Biomed. Pharmacother. 2005; 59: 64–69.

Radford D. Side effects of verapamil in infants. Arch. Dis. Child. 1983; 58: 465–466.

Roelofsen H, Vos TA, Schippers IJ, Kuipers F, Koning H, Moshage H, Jansen PL, Muller M. Increased levels of the multidrug resistance protein in lateral membranes of

proliferating hepatocyte-derived cells. Gastroenterology. 1997; 112: 511–521.

Ross JA, Kasum CM. Dietary flavonoids: bioavailability, metabolic effects, and safety. Annu. Rev. Nutr. 2002; 22: 19–34.

Saitoh H, Aungst BJ. Possible involvement of multiple P-glycoprotein-mediated efflux systems in the transport of verapamil and other organic cations across rat intestine. Pharm. Res. 1995; 12: 1304–1310.

Schaub TP, Kartenbeck J, Konig J, Spring H, Dorsam J, Staehler G, Storkel S, Thon WF, Keppler D. Expression of the MRP2 gene-encoded conjugate export pump in human kidney proximal tubules and in renal cell carcinoma. J. Am. Soc. Nephrol. 1999; 10: 1159–1169.

Schomerus M, Spiegelhaider B, Stieren B, Eichelbaum M. Physiologic disposition of verapamil in man. Cardiovasc. Res. 1976; 10: 605–612.

Schuetz EG, Beck WT, Schuetz JD. Modulators and substrates of P-glycoprotein and cytochrome P4503A coordinately up-regulate these proteins in human colon carcinoma cells. Mol. Pharmacol. 1996; 49: 311–318.

Skach WR, Calayag MC, Lingappa VR. Evidence for an alternate model of human P-glycoprotein structure and biogenesis. J. Biol. Chem. 1993; 268: 6903–6908.

Silverman JA, Raunio H, Gant TW, Thorgeirsson SS. Cloning and characterization of a member of the rat multidrug resistance (mdr) gene family. Gene. 1991; 106: 229–236

Spencer JP, Chowrimootoo G, Choudhury R, Debnam ES, Srai SK, Rice-Evans CA. The small intestine can both absorb and glucuronidate luminal flavonoids. FEBS Lett. 1999; 458: 224–230.

Spencer JP, Schroeter H, Crossthwaithe AJ, Kuhnle G, Williams RJ, Rice-Evans C. Contrasting influences of glucuronidation and O-methylation of epicatechin on hydrogen peroxide-induced cell death in neurons and fibroblasts. Free Radic. Biol. Med. 2001; 31: 1139–1146.

Sutherland L, Ebner T, Burchell B. The expression of UDP-glucuronosyltransferases of the UGT1 family in human liver and kidney and in response to drugs. Biochem. Pharmacol. 1993; 45: 295–301.

Taipalensuu J, Tornblom H, Lindberg G, Einarsson C, Sjoqvist F, Melhus H, Garberg P, Sjostrom B, Lundgren B, Artursson P. Correlation of gene expression of ten drug efflux proteins of the ATP-binding cassette transporter family in normal human jejunum and in human intestinal epithelial Caco-2 cell monolayers. J. Pharmacol. Exp.

Ther. 2001; 299: 164–170.

Thiebaut F, Tsuruo T, Hamada H, Gottesman MM, Pastan I, Willingham MC. Cellular localisation of the multidrug-resistance gene product P-glycoprotein in normal human tissues. Proc. Natl. Acad. Sci. 1987; 84: 7735–7738.

Tsai TH, Liu MC. Determination of extracellular hesperidin in blood and bile of anaesthetized rats by microdialysis with high-performance liquid chromatography: a pharmacokinetic application. J. Chromatogr. B. Analyt. Technol. Biomed. Life. Sci. 2004; 806: 161–166.

Turgeon D, Carrier JS, Levesque E, Hum DW, Belanger A. Relative enzymatic activity, protein stability, and tissue distribution of human steroid-metabolizing UGT2B subfamily members. Endocrinology. 2001; 142: 778–787.

Van der Bliek AM, Kooiman PM, Schneider C, Borst P. Sequence of mdr3 cDNA encoding a human P-glycoprotein. Gene. 1988; 71; 401–411

Wacher VJ, Silverman JA, Zhang Y, Benet LZ. Role of P-glycoprotein and cytochrome P450 3A in limiting oral absorption of peptides and peptidomimetics, J. Pharm. Sci. 1998; 87: 1322–1330.

Wacher VJ, Wu CY, Benet LZ. Overlapping substrate specificities and tissue distribution of cytochrome P450 3A and P-glycoprotein: implications for drug delivery and activity in cancer chemotherapy. Mol. Carcinog. 1995; 13: 129–134.

Wang JS, Ruan Y, Taylor RM, Donovan JL, Markowitz JS DeVane CL. The brain entry of risperidone and 9-hydroxyrisperidone is greatly limited by P-glycoprotein. Int. J. Neuropsychopharmacol. 2004; 7: 415–419.

Watkins PB. Drug metabolism by cytochromes P450 in the liver and small bowel. Gastrointest. Pharmacol. 1992; 21: 511–526.

Watkins PB. The barrier function of CYP3A4 and P-glycoprotein in the small bowel, Adv. Drug Deliv. Rev. 1997; 27: 161–170.

Wrighton SA. The human CYP3A subfamily: practical considerations. Drug Metab. Rev. 2000; 32: 339–361

Yoshimura A, Kuwazuru Y, Sumizawa T, Ichikawa M, Ikeda S. Cytoplasmic orientation and two-domain structure of the multidrug transporter, P-glycoprotein, demonstrated with sequence-specific antibodies. J. Biol. Chem. 1989; 264: 16282–16291

Zaman GJ, Versantvoort CH, Smit JJ, Eijdems EW, De Haas M, Smith AJ, Broxterman HJ, Mulder NH, De Vries EG, Baas F. Analysis of the expression of MRP, the gene for a

new putative transmembrane drug transporter, in human multidrug resistant lung cancer cell lines. Cancer Res. 1993; 53: 1747–1750.

van Zanden JJ, Wortelboer HM, Bijlsma S, Punt A, Usta M, Bladeren PJ, Rietjens IM, Cnubben NH. Quantitative structure activity relationship studies on the flavonoid mediated inhibition of multidrug resistance proteins 1 and 2. Biochem. Pharmacol. 2005; 69: 699–708.

Zhang JT, Ling V. Study of membrane orientation and glycosylated extracellular loops of mouse P-glycoprotein by *in vitro* translation. J. Biol. Chem. 1991; 266: 18224–18232.

Zhang S, Morris ME. Effects of the flavonoids biochanin A, morin, phloretin, and silymarin on P-glycoprotein-mediated transport. J. Pharmacol. Exp. Ther. 2003a; 304: 1258–1267.

Zhang S, Morris ME. Effect of the flavonoids biochanin A and silymarin on the P-glycoprotein-mediated transport of digoxin and vinblastine in human intestinal Caco-2 cells. Pharm. Res. 2003b; 20: 1184–1191.

감사의 글

석사학위를 받은 후 10 년의 공백으로 다시 대학원 진학의 용기를 갖도록 격려해주시고, 본 논문의 연구계획에서부터 완성까지 학문적인 기틀과 소상한 가르침을 주신 지도교수이신 최준식 교수님께 깊은 감사를 드립니다.

그리고 약제학교실의 박영길 선생님, 동료, 후배, 수업을 통해 가르침을 주신 교수님들께 감사 드립니다.

특히 못난 딸을 위해 많은 희생을 아끼지 않으신 우리엄마 너무죄송하고 고맙고, 말없이 아내의 늦깎이 공부를 지켜봐 주었던 사랑하는 남편, 믿음직하게 자라준 아들 환민, 사랑하는 딸 현정, 항상 나에게 기쁨을 주는 딸 채원, 우리 가족 모두에게 고맙습니다.

아울러 저에게 많은 관심을 베풀어주신 전남대학교병원 약제부 직원들과 과정을 마칠 수 있도록 배려해주신 모든 분들과 함께 기쁨을 나누고 싶습니다.

끝으로 더욱 발전하는 저의 모습을 지켜봐 주시기 바랍니다.

저작물 이용 허락서

학 과	약학과	학 번	20057392	과 정	박사
성 명	한 글 : 윤재경 한 문 : 尹在京 영 문 : Yun Jae Kyoung				
주 소	광주 서구 화정동 400-6 꽃담마을 대림 이편한세상 103-1803				
연락처	E-mail : happykid@hanmail.net				
논문제목	한글: 흰쥐에서 헤스페리딘 또는 에피게로카테친이 베라파밀의 경구생체이용율에 미치는 영향 영문: Effects of Hesperidin or Epigallocatechin gallate on the Oral Bioavailability of Verapamil in Rats				

본인이 저작한 위의 저작물에 대하여 다음과 같은 조건아래 조선대학교가 저작물을 이용할 수 있도록 허락하고 동의합니다.

- 다 음 -

1. 저작물의 DB 구축 및 인터넷을 포함한 정보통신망에의 공개를 위한 저작물의 복제, 기억장치에의 저장, 전송 등을 허락함
2. 위의 목적을 위하여 필요한 범위 내에서의 편집·형식상의 변경을 허락함. 다만, 저작물의 내용변경은 금지함.
3. 배포·전송된 저작물의 영리적 목적을 위한 복제, 저장, 전송 등은 금지함.
4. 저작물에 대한 이용기간은 5 년으로 하고, 기간종료 3 개월 이내에 별도의 의사표시가 없을 경우에는 저작물의 이용기간을 계속 연장함.
5. 해당 저작물의 저작권을 타인에게 양도하거나 또는 출판을 허락을 하였을 경우에는 1 개월 이내에 대학에 이를 통보함.
6. 조선대학교는 저작물의 이용허락 이후 해당 저작물로 인하여 발생하는 타인에 의한 권리 침해에 대하여 일체의 법적 책임을 지지 않음
7. 소속대학의 협정기관에 저작물의 제공 및 인터넷 등 정보통신망을 이용한 저작물의 전송·출력을 허락함.

동의여부 : 동의 (√) 반대 ( )

2008 년 02 월

저작자: 윤재경 (인)

조선대학교 총장 귀하